

CHARACTERISTICS OF INTERDIGITAL LINE

BY MRS. ALAKANANDA PAUL

(Department of Electrical Communication Engineering, Indian Institute of Science, Bangalore-12)

(Received on April 28, 1964)

ABSTRACT

The characteristics of a planar interdigital line constructed in the Laboratory have been evaluated by using available existing relations based on waveguide approach as well as bar line theory. The results are presented graphically.

INTRODUCTION

Interdigital lines¹⁻⁴ are extensively used in the construction of M-Carri-notrons and other forward and backward wave amplifiers due to their broadband characteristics, high power handling capacity, and the ease with which they can be matched to a coaxial line or a waveguide. The important parameters of an interdigital line are delay ratio ($\tau = c/v_p$), interaction impedance (k) and dispersion factor (v_p/v_g). These parameters depend on the frequency of operation, periodicity of the structure (p), distance between top and bottom plates (w), distance between the fingers and the grounded plate (b), spacing between any two fingers (m), the distance between the tip of a fingers and wall opposite (g), the width of the fingers (d), length of the fingers (l) and the thickness of the fingers (t).

The object of this paper is to present graphically the characteristics of a planar interdigital line for S-band (Figs. I and II) which has been constructed in the laboratory. The calculations have been made from the existing relations obtained on the basis of waveguide approach⁴. Some of the characteristics have also been calculated by applying the results obtained from the bar line theory^{1, 3}, and the results have been compared with those obtained from the waveguide approach. The variations of delay ratio (τ), delayed wavelength for first reverse space harmonic (λ_{-1}), characteristic impedance (Z_0), interaction impedance for first reverse space harmonic (K_{-1}), dispersion factor (v_p/v_g) and low frequency cut off wavelength (λ_1) as a function of p , W and λ_0 (free space wavelength) have been calculated and the results are presented graphically. It is believed that these graphs will serve as ready reference for the purpose of designing interdigital lines.

THEORETICAL RELATIONS

Waveguide approach. In order to analyse the characteristics of the interdigital line the structure is assumed⁴ to consist of three different regions.

The first region consists of the space between the backwall and the interdigital structure. The second region is the interdigital structure. The third region is the interaction space. The fields in first and third regions are assumed to consist of TE waveguide modes. The second region is considered to be equivalent to a number of parallel plate capacitor with uniform field distribution between the fingers and fringing field on both sides.

The analysis by Moats⁴ leads to the following characteristic equation

$$rp (\coth rb + S) + r^2 p^2 L = \beta_0^2 w^2 \left(C - \frac{p^2}{w^2} L \right) \quad [1]$$

where

$$\beta^2 = \gamma^2 + \beta_0^2, \quad \beta_0^2 = \omega^2 \mu \epsilon$$

$$S = \frac{w}{f} + \frac{2\gamma w}{f} \sum_{s=1}^{\infty} \frac{1}{\gamma_s} \left(\frac{\sin \frac{1}{2} \beta_s w}{\frac{1}{2} \beta_s w} \right)^2. \quad [2]$$

In the usual range of operation $S \approx 1 - \frac{0.615}{\gamma w}$.

$$C = \frac{t}{m} + \frac{1}{\pi} \left(\frac{1}{\alpha} \ln \frac{1+\alpha}{1-\alpha} + \ln \frac{1-\alpha}{\alpha^2} \right)$$

$$L = \frac{t}{m} + \frac{1}{\pi} \left[\left(\alpha + \frac{1}{\alpha} \right) \ln \frac{1+\alpha}{1-\alpha} - 2 \ln \frac{4\alpha}{1-\alpha^2} \right]$$

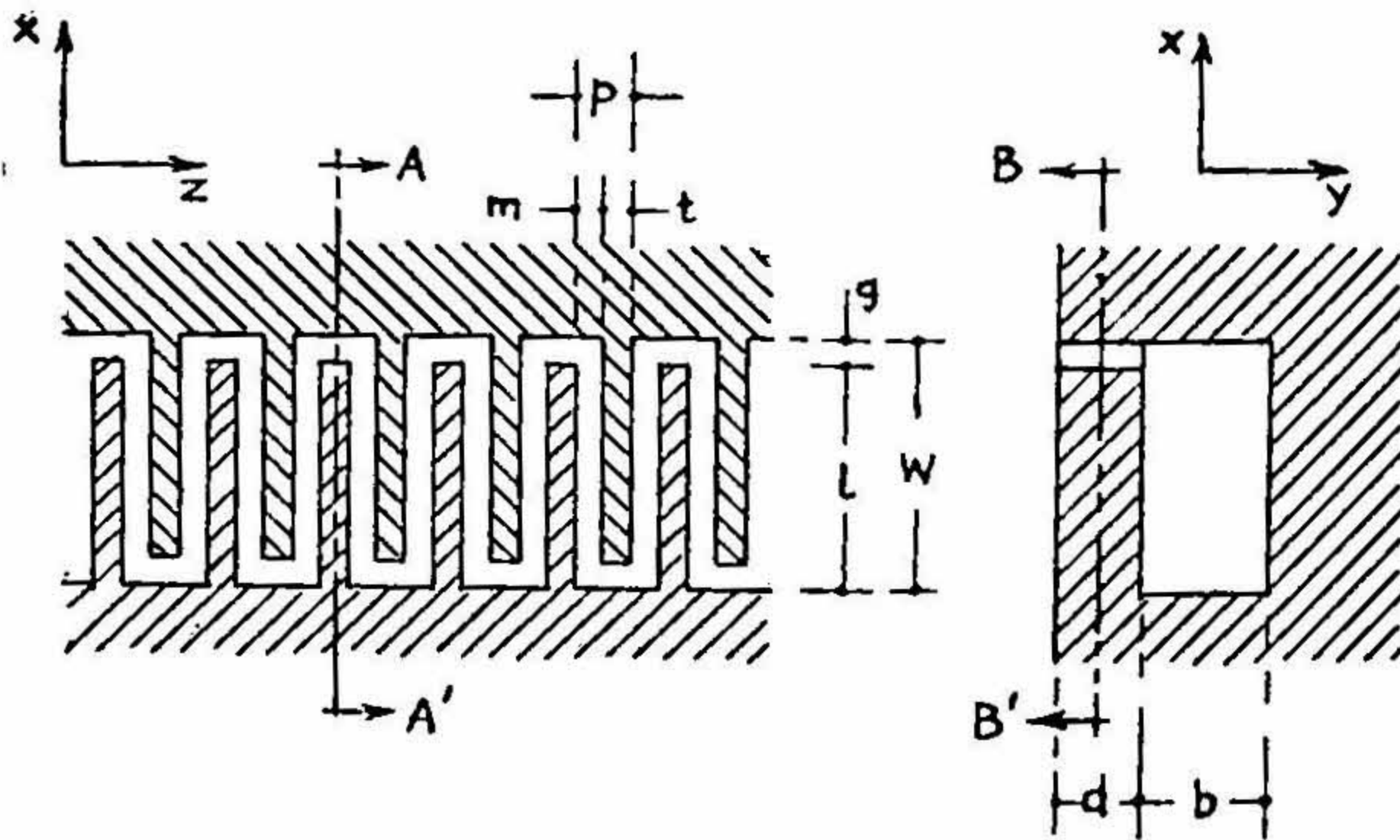


FIG. 1.
An interdigital line

The propagation constant γ is calculated from equation [1] and hence β is calculated from equation [2]. The phase constant β_n for the n th space harmonic is given by the relation

$$\beta_n = \beta + (2n + 1) \pi/p \quad [3]$$

For the first reverse space harmonic $n = -1$

$$\beta_{-1} = \beta - \pi/p \quad [4]$$

The phase velocity v_p for the first reverse space harmonic is calculated from the relation

$$V_p = \frac{\omega}{|\beta_{-1}|} \quad [5]$$

The delay ratio (τ) and the delayed wavelength (λ_{-1}) are calculated respectively from the following relations

$$\tau = \frac{C}{V_p} = \frac{|\beta_{-1}|}{\beta_0} \quad [6]$$

and

$$\lambda_{-1} = \frac{2\pi}{|\beta_{-1}|} \quad [7]$$

The group velocity v_g is obtained from

$$V_g = \frac{\omega}{\beta} \left[1 - \frac{1}{2} \cdot \frac{\beta p (\coth \beta b + S) + \beta^2 p b \operatorname{cosech}^2 \beta b - 0.615 p/w}{\beta^2 p^2 L + \beta p (\coth \beta b + s)} \right] \quad [8]$$

Hence, the dispersion factor (v_p/v_g) can be calculated from the relations [5] and [8].

The characteristic impedance (Z_0) and interaction impedance (K_{-1}) are given by the relations

$$Z_0 = \sqrt{\frac{\mu_0}{\epsilon_0} \cdot \frac{p}{w} \cdot \frac{1}{C} \cdot \frac{c}{v_g}} \quad [9]$$

$$K_{-1} = Z_0 \left[\frac{1}{\beta_{-1} p} \cdot \frac{\sin \frac{1}{2} \beta_{-1} m}{\frac{1}{2} \beta_{-1} m} \right]^2 \quad [10]$$

Bar Line Approach. The interdigital line is considered^{1, 2, 3} as a set of parallel bar of length l connected to the ground alternately at one end or other (Fig. II).

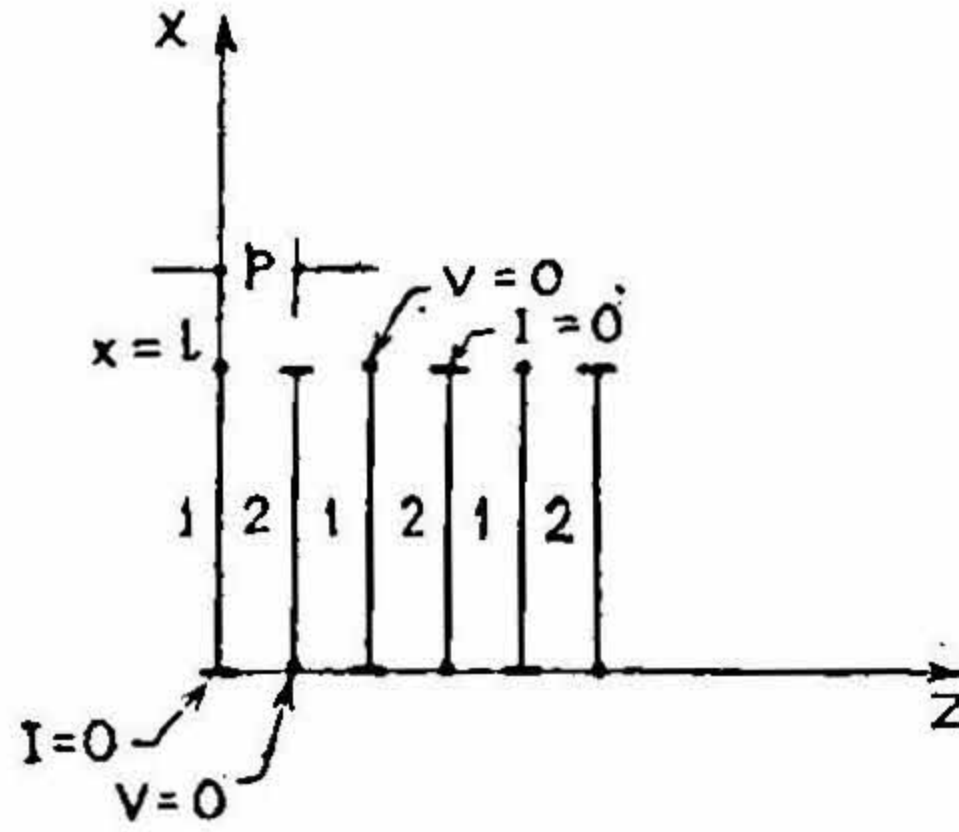


FIG. II

Interdigital line as a set of parallel bars alternatively short circuited to ground and open circuited

In this case, one can show that

$$\tan^2 \frac{\pi l}{\lambda} = \frac{Y(\psi/2)}{Y(\psi/2 + \pi)} \quad [11]$$

where

$$\psi = 2\beta p$$

In case where all the the capacities are neglected except between adjacent fingers (γ'), we have

$$\psi = \frac{4\pi l}{\lambda} \quad [12]$$

This phase shift corresponds to a TEM wave moving in a zigzag fashion between the combs and high frequency cut off occurs at $\lambda = 2l$.

However, if we consider the presence of a grounded plate, we have to include γ_0 , the capacity between a finger and ground. Thus eq. [11] can be written as,

$$\tan^2 \frac{\pi l}{\lambda} = \frac{\gamma_0 + 4\gamma' \sin^2 \psi/4}{\gamma_0 + 4\gamma' \cos^2 \psi/4} \quad [13]$$

from which ψ can be calculated.

In this case, the cut off wavelengths λ_1 and λ_2 can be calculated by putting $\psi = 0$ and $\psi = 2\pi$

λ_1 and λ_2 are related by

$$\frac{1}{\lambda_1} + \frac{1}{\lambda_2} = \frac{1}{2l} \quad [14]$$

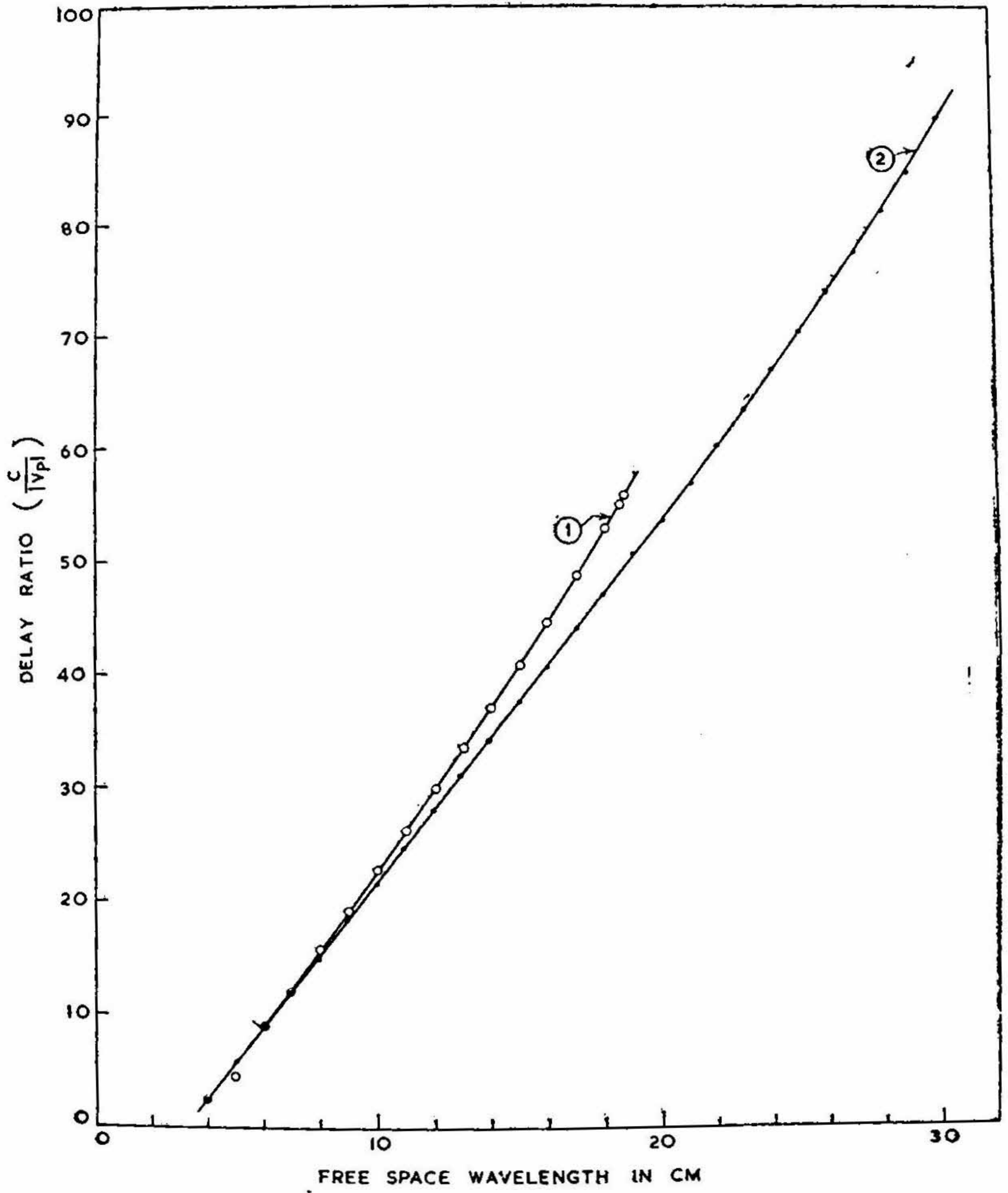


FIG. III

Delay ratio as a function of free-space wavelength.
 $p=0.165$ cm, $w=1.628$ cm, $m=0.11$ cm, $b=0.159$ cm,
 $g=0.119$ cm, $l=1.509$ cm, $d=0.278$ cm, $t=0.055$ cm.
 $\alpha=0.667$

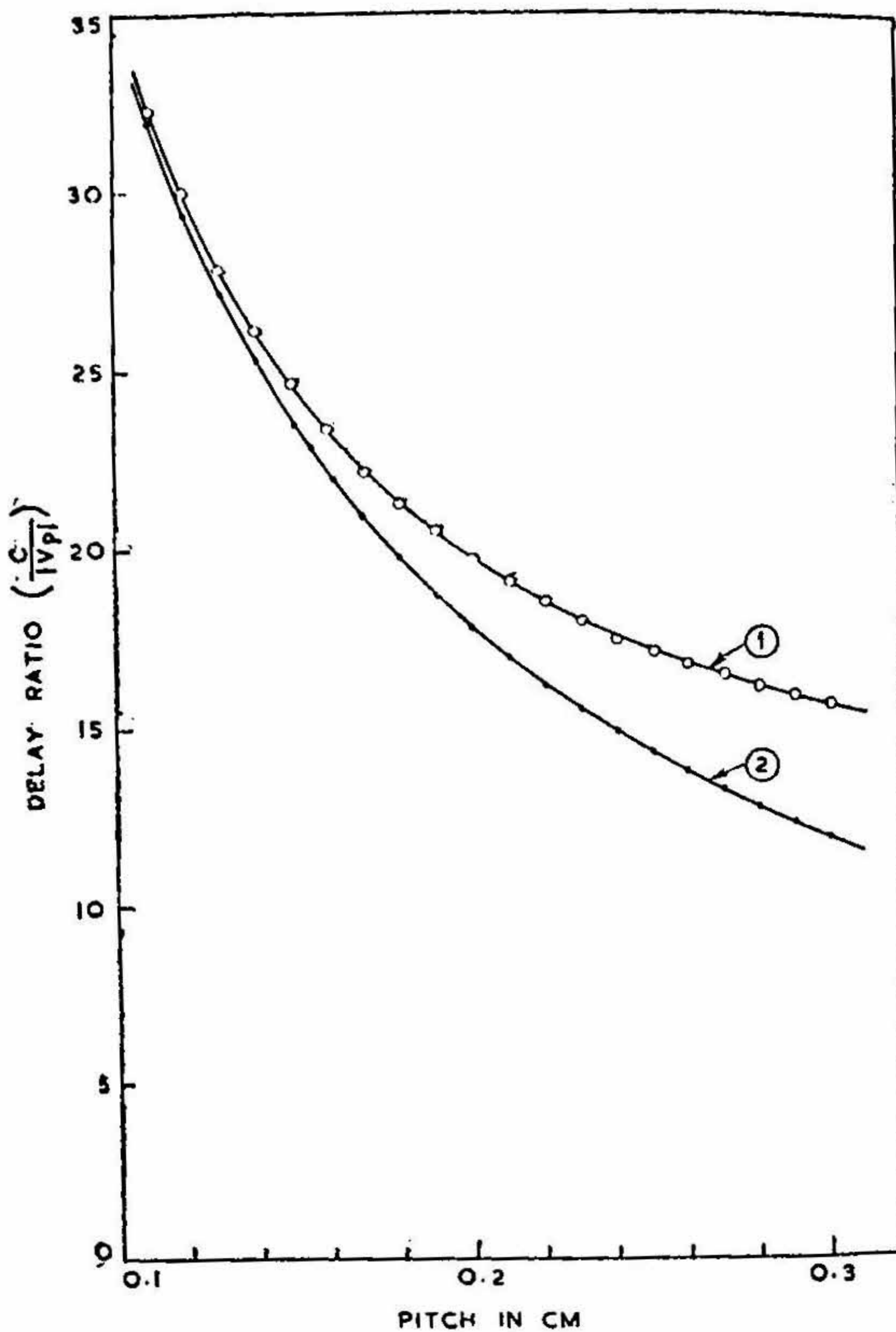


FIG. IV

Delay ratio as a function of pitch
 $\lambda_0 = 10$ cm; $w = 1.628$ cm, $b = 0.159$ cm, $g = 3.119$ cm;
 $l = 1.539$ cm, $d = 0.278$ cm, $t = 0.055$ cm.

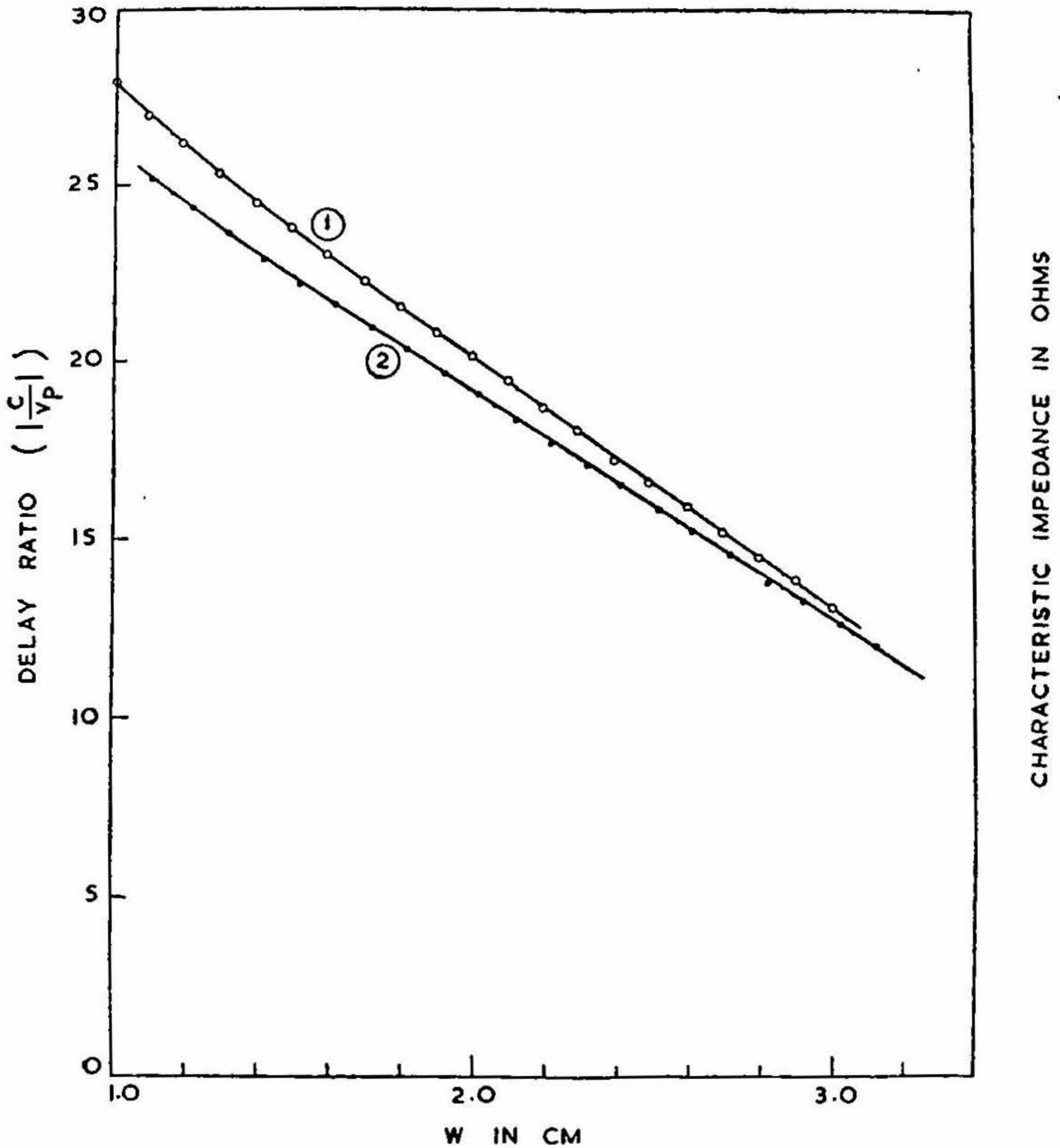


FIG. V

Delay ratio as a function of distance between top and bottom plates

$$\lambda_0=10 \text{ cm, } \quad p=0.165 \text{ cm, } \quad m=0.11 \text{ cm, } \quad b=0.159 \text{ cm,}$$

$$g=0.119 \text{ cm, } \quad d=0.278 \text{ cm, } \quad t=0.055 \text{ cm, } \quad \alpha=0.667.$$

From ψ , β_n for n th space harmonic can be calculated using the relation

$$\beta_n = \frac{\psi + 2n\pi}{2p} \quad [15]$$

knowing β_n , delay ratio and delayed wavelength for n th space harmonic can be calculated.

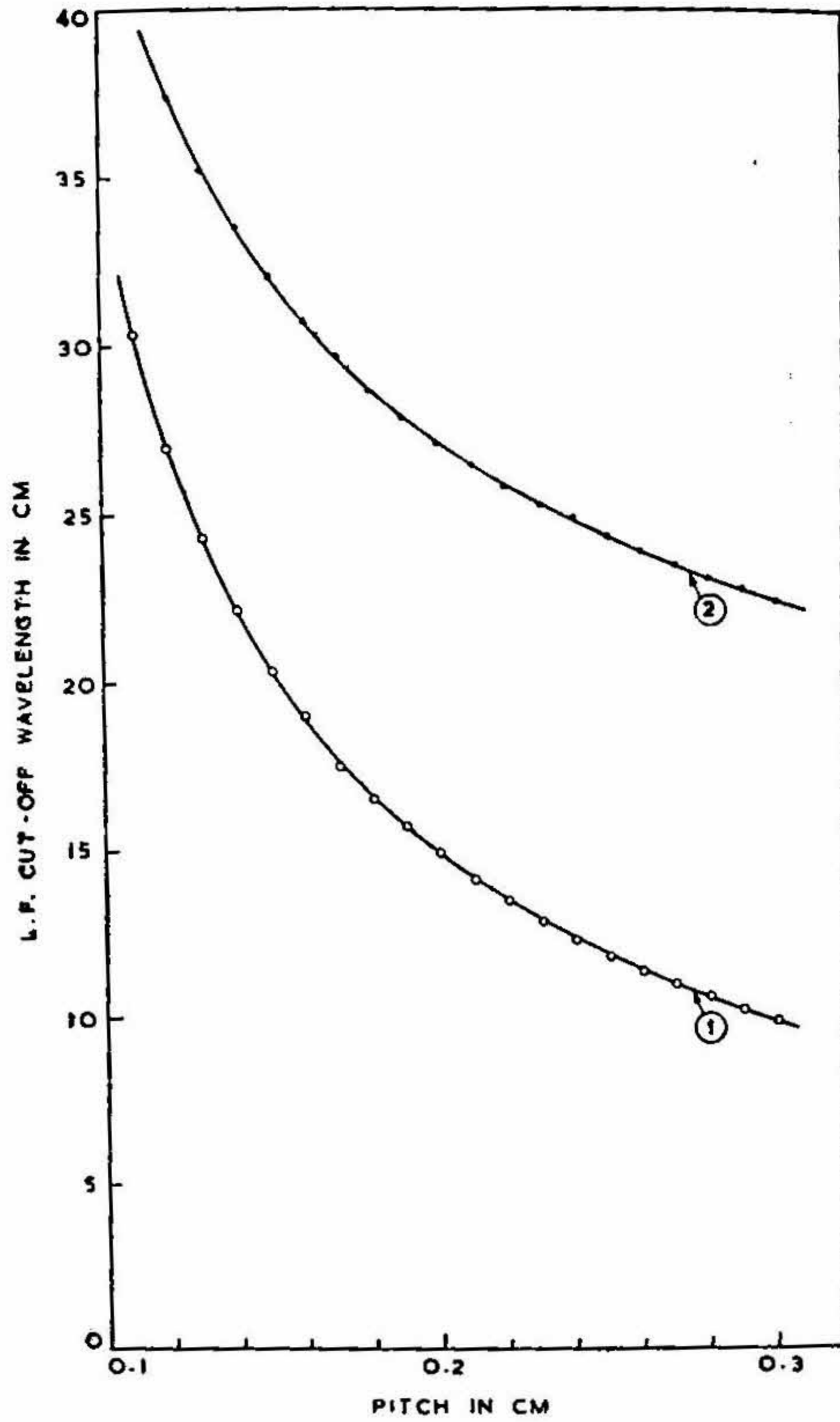


FIG. VI

Low frequency cut off wavelength as a function of pitch.
 $\lambda_0 = 10$ cm, $w = 1.628$ cm, $b = 0.159$ cm, $g = 0.119$ cm,
 $l = 1.509$ cm, $d = 0.278$ cm, $t = 0.055$ cm.

When the effect of the grounded plate is neglected, the delay ratio for the first reverse space harmonic is given by the simple relation

$$\frac{c}{v_p} = \frac{l}{p} - \frac{\lambda}{2p}$$

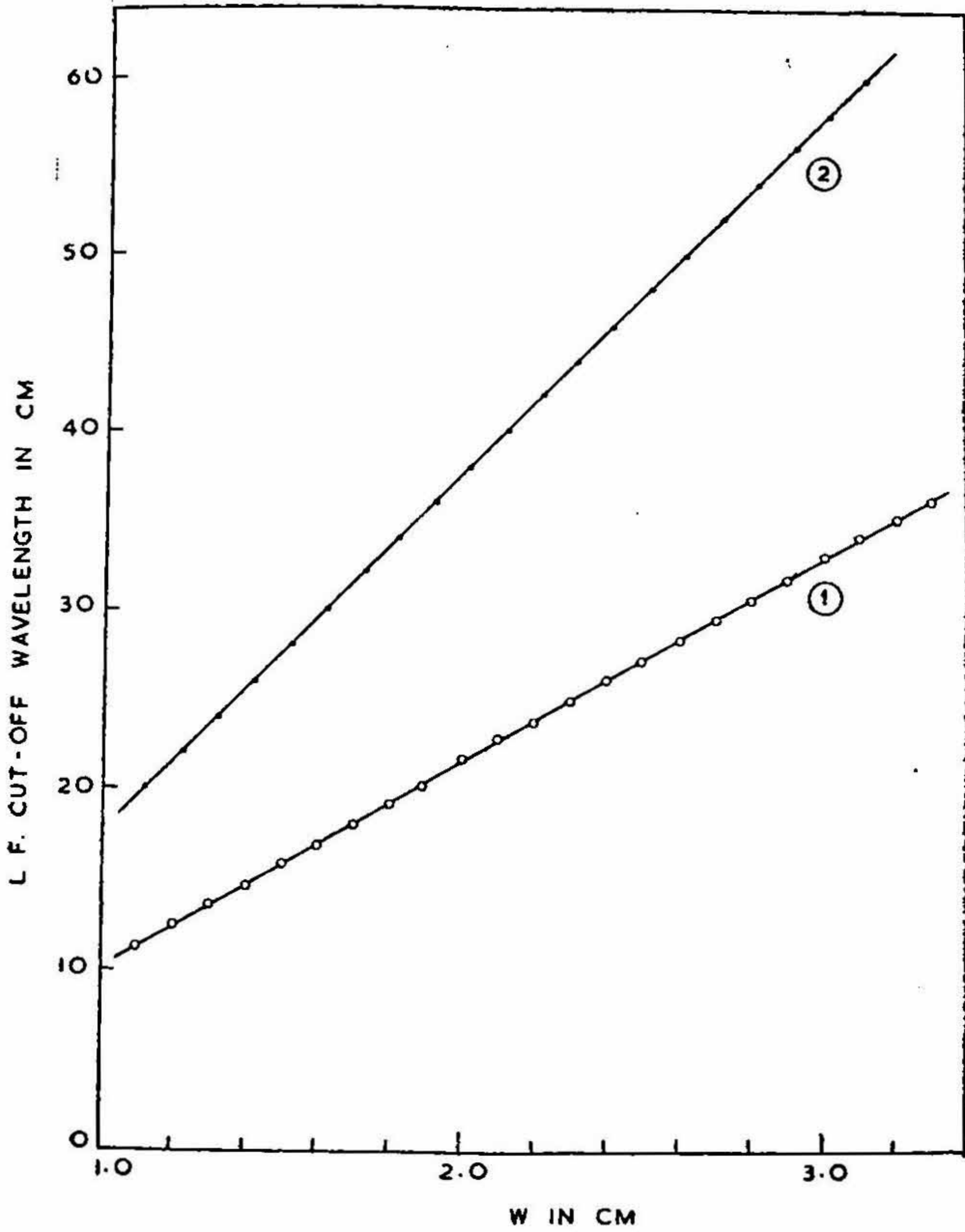


FIG VII

Low frequency cut off wavelength as a function of distance between top and bottom plates
 $\lambda_0=10$ cm, $p=0.165$ cm, $m=0.11$ cm, $b=0.159$ cm,
 $g=0.119$ cm, $d=0.278$ cm, $t=0.055$ cm. $\alpha=0.667$

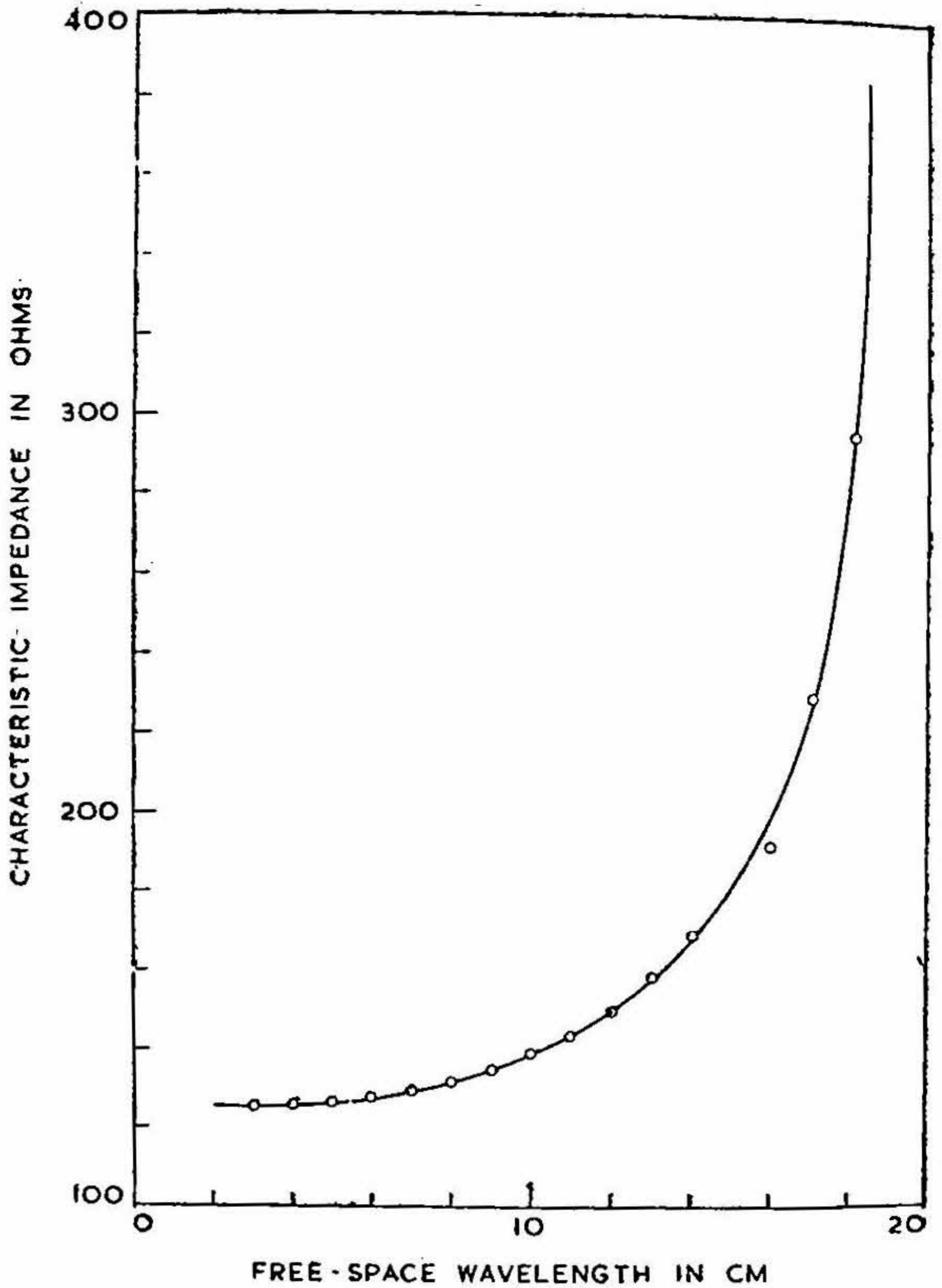


FIG. VIII

Characteristic impedance as a function of free space wavelength

$p=0.165$ cm, $w=1.628$ cm. $m=0.11$ cm, $b=0.159$ cm,
 $g=0.119$ cm, $l=1.509$ cm. $d=0.278$ cm. $t=0.055$ cm,
 $\alpha=0.667$.

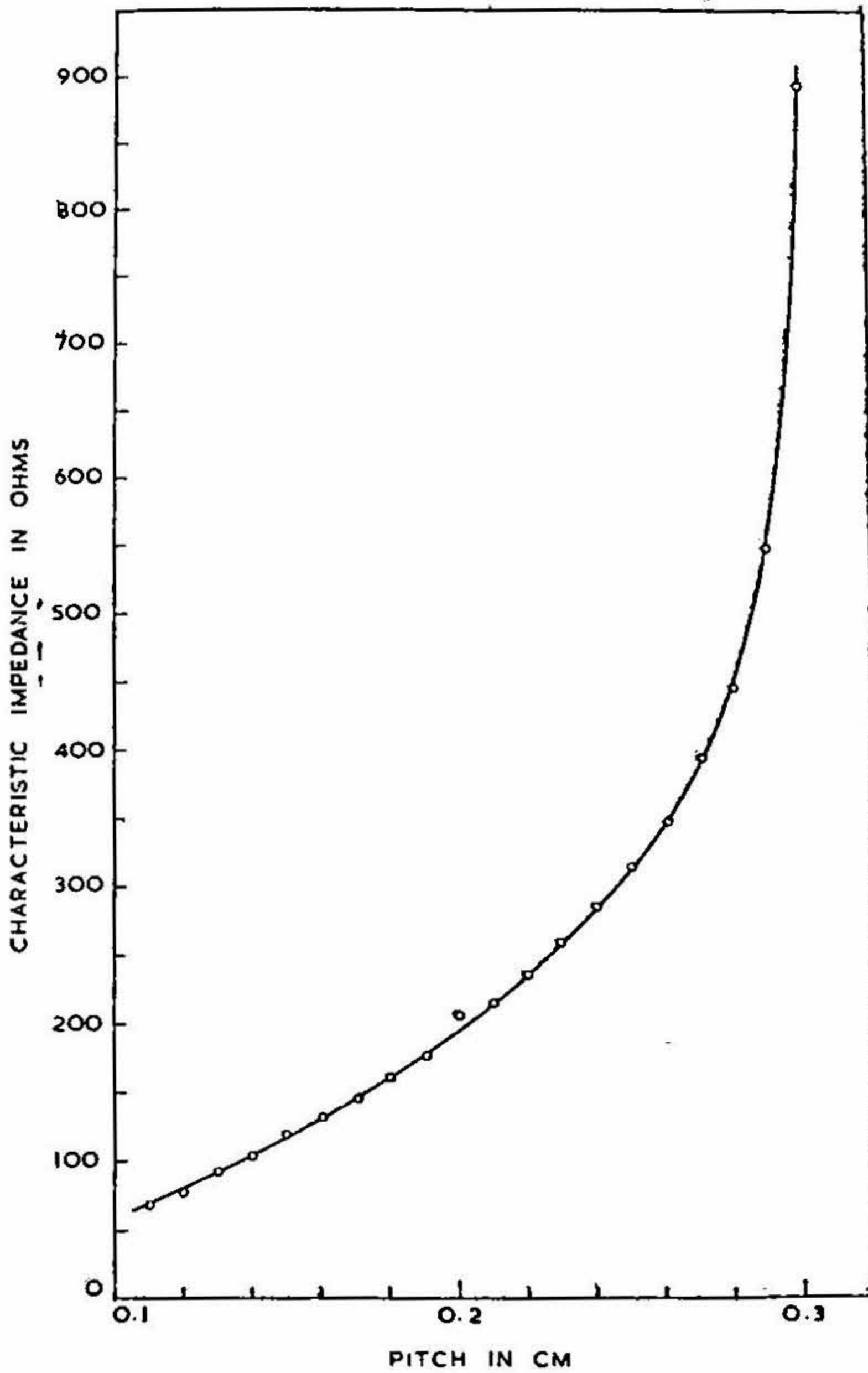


FIG. IX

Characteristic impedance as a function of pitch
 $\lambda_0=10$ cm, $w=1.628$ cm. $b=0.159$ cm, $g=0.119$ cm.
 $l=1.509$ cm, $d=0.278$ cm. $t=0.055$ cm.

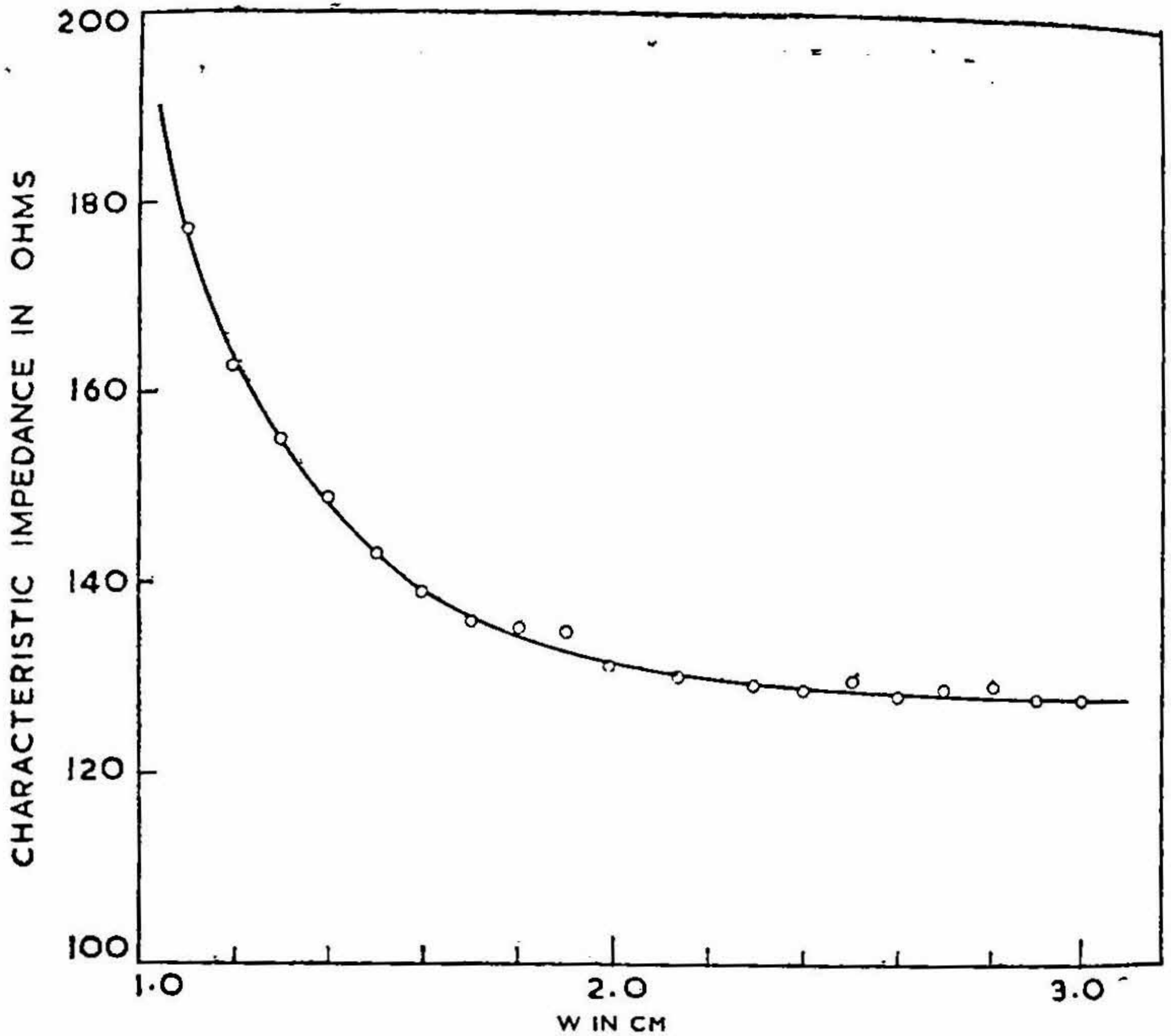


FIG. X

Characteristic impedance as a function of distance between top and bottom plates
 $\lambda_0=10$ cm, $p=0.165$ cm., $m=0.11$ cm, $b=0.159$ cm,
 $g=0.119$ cm, $d=0.278$ cm., $t=0.055$ cm, $\alpha=0.667$.

DESIGN CHARACTERISTICS

The dimensions of the interdigital line constructed in the laboratory are as follows : —

Pitch, p	0.165 cm
Distance between top and bottom plates W	1.628 cm
Width of the gap between fingers m	0.11 cm
Distance between fingers and the ground plate b	0.159 cm
Distance between the tip of a finger and wall opposite g	0.119 cm
Length of the fingers l	1.509 cm
Width of the fingers d	0.278 cm
Thickness of the fingers t	0.055 cm
Ratio of gap width to pitch α	0.667

The operating frequency is 3 KMc/s

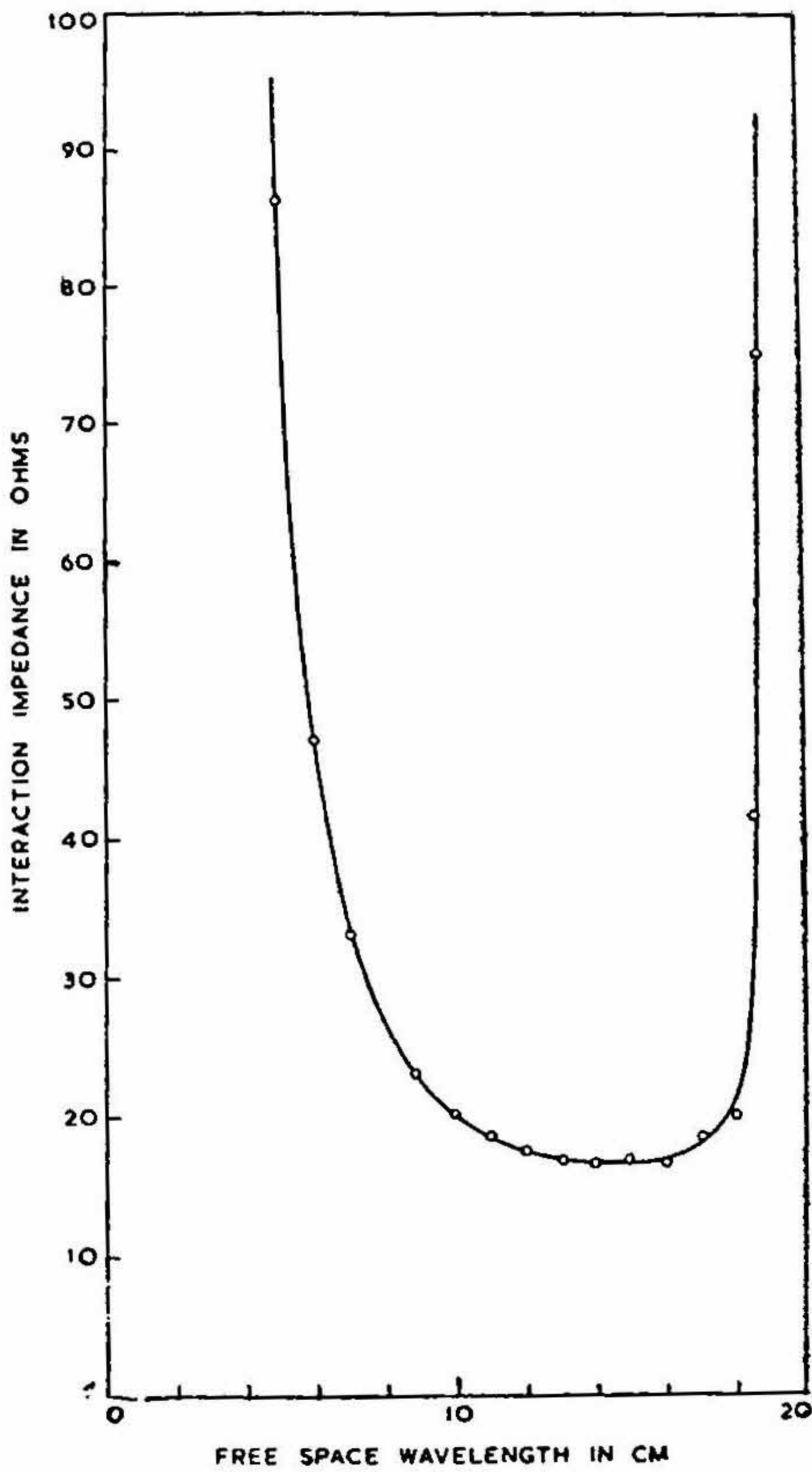


FIG. XI

Interaction impedance as a function of free-space wave length.
 $p=0.165$ cm, $w=1.628$ cm, $m=0.11$ cm, $b=0.159$ cm,
 $g=0.119$ cm, $l=1.509$ cm, $d=0.278$ cm, $t=0.055$ cm,
 $\alpha=0.667$.

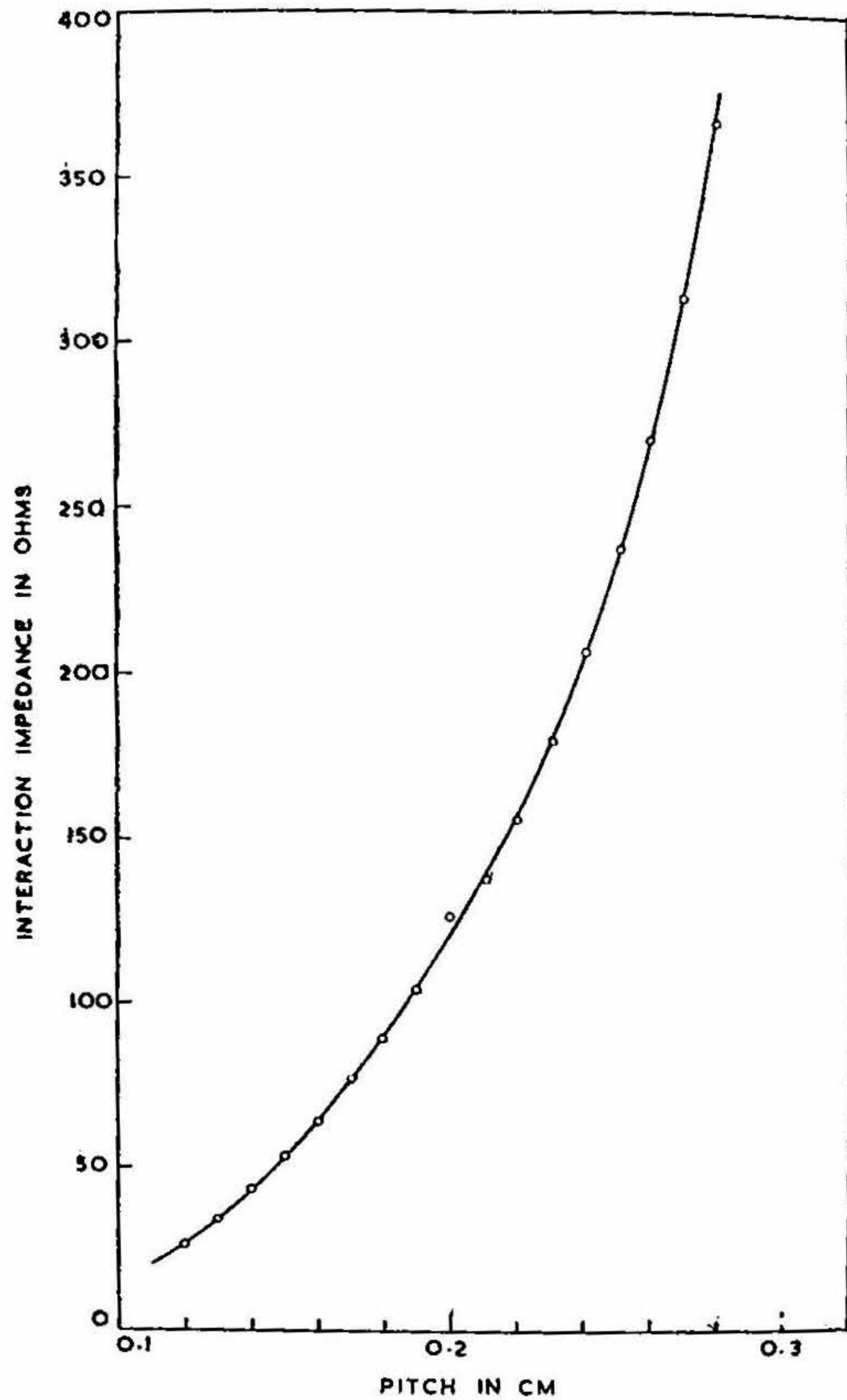


FIG XII

Interaction impedance as a function of pitch.

$\lambda_0 = 10$ cm., $w = 1.628$ cm., $b = 0.159$ cm., $g = 0.119$ cm.
 $l = 1.509$ cm., $d = 0.278$ cm., $t = 0.055$ cm.

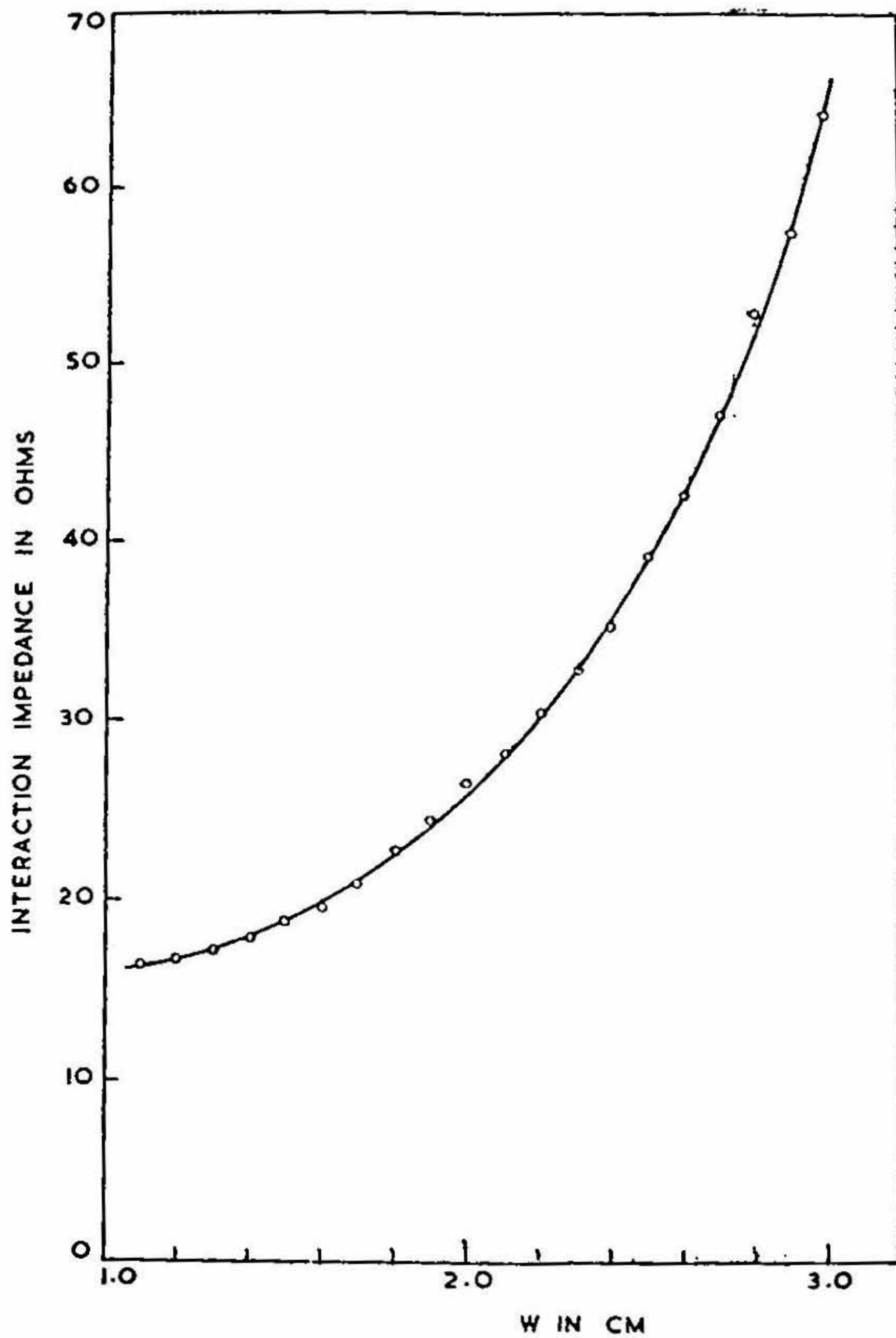


FIG. XIII

Interaction impedance as a function of distance between top and bottom plates.
 $\lambda_0 = 10$ cm., $p = 0.165$ cm., $m = 0.11$ cm., $b = 0.159$ cm., $g = 0.119$ cm.
 $d = 0.278$ cm., $t = 0.055$ cm., $\alpha = 0.667$.

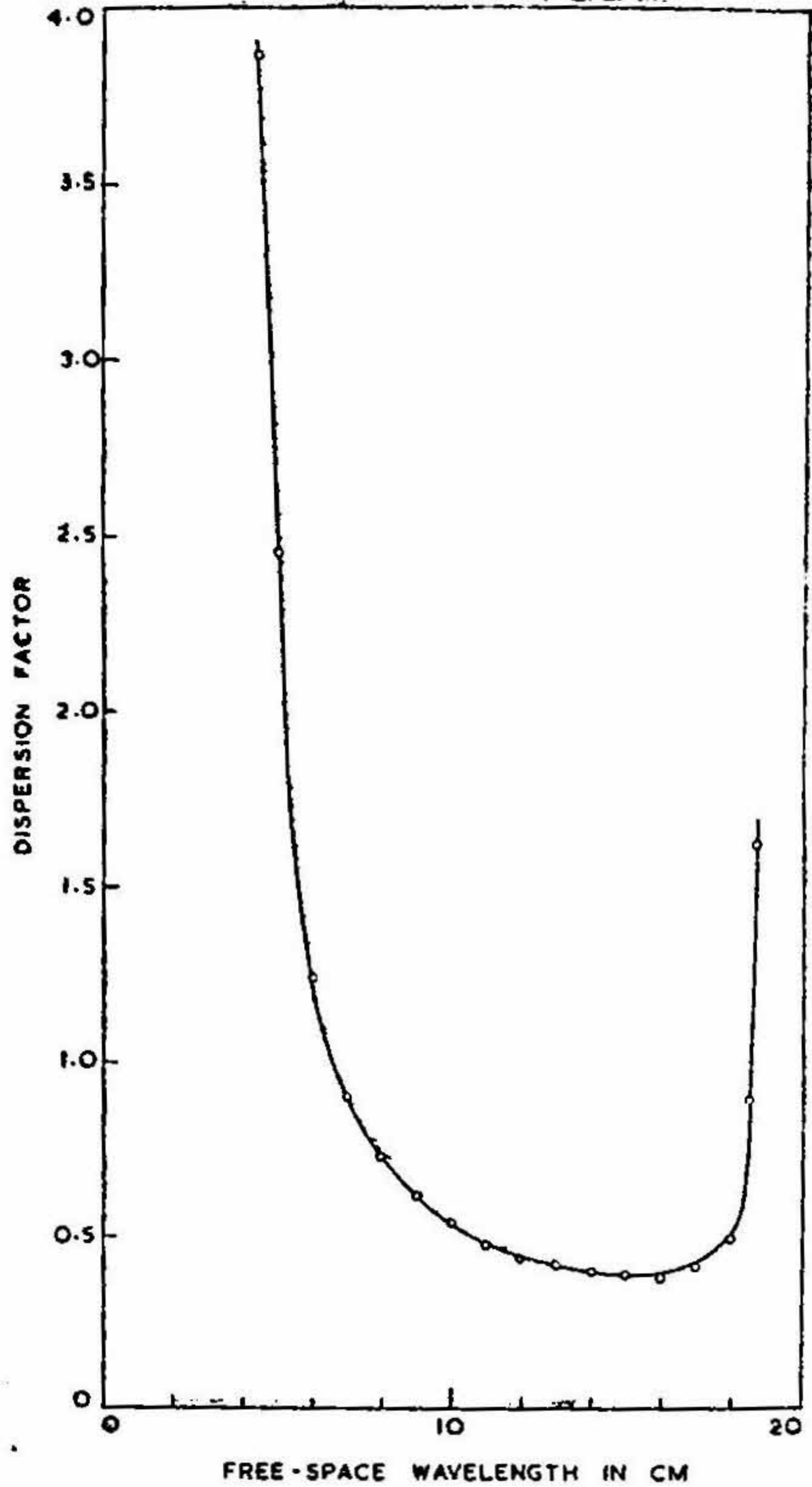


FIG. XIV

Dispersion factor as a function of free space wavelength.
 $p=0.165$ cm., $w=1.628$ cm., $m=0.11$ cm, $b=0.159$ cm.
 $g=0.119$ cm., $l=1.509$ cm., $d=0.278$ cm., $t=0.055$ cm.
 $\alpha=0.667$.

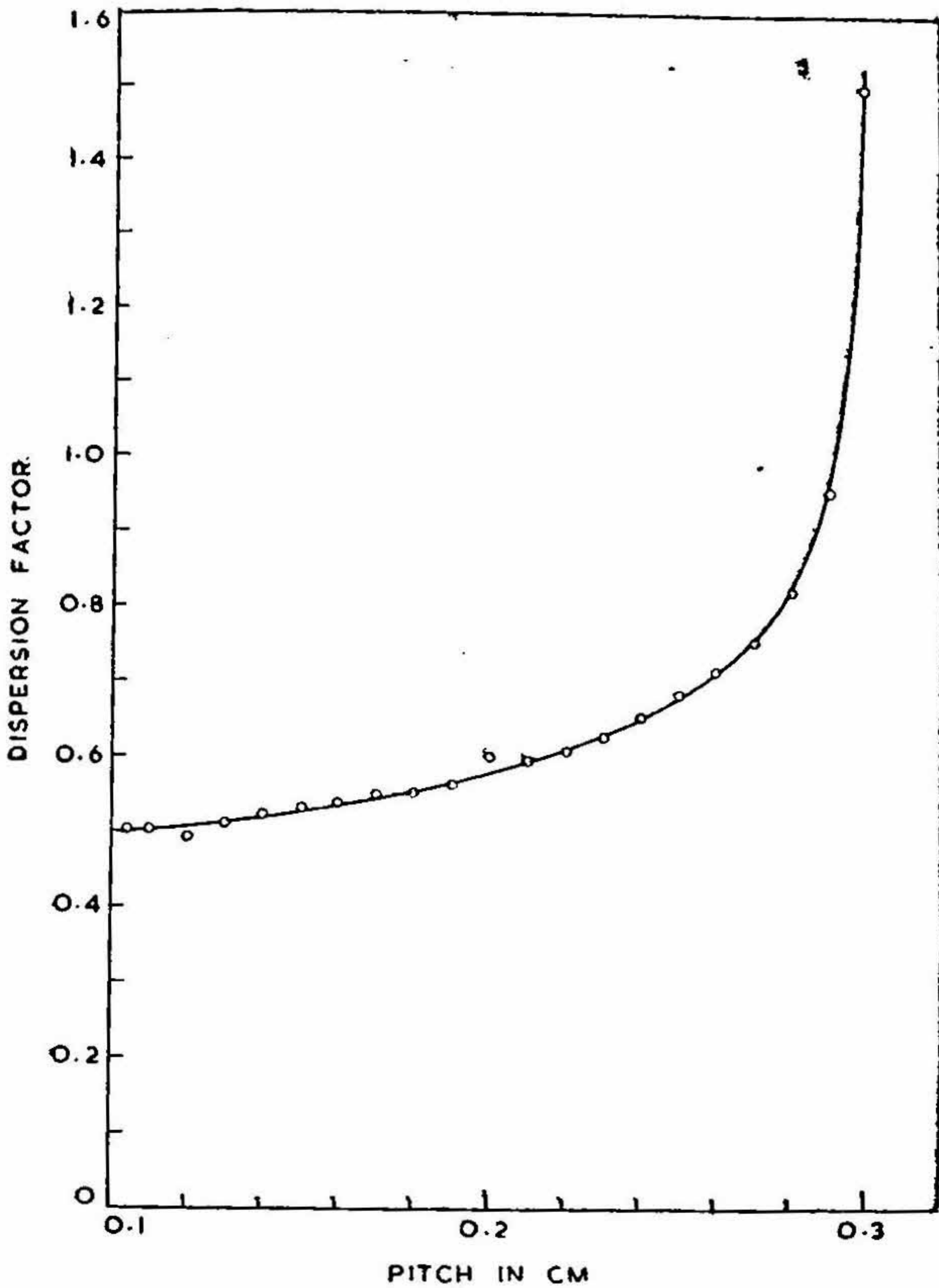


FIG. XV

Dispersion factor as a function of pitch.

$\lambda_0 = 10$ cm., $w = 1.628$ cm., $b = 0.159$ cm., $g = 0.119$ cm.,
 $l = 1.509$ cm., $d = 0.278$ cm., $t = 0.055$ cm.

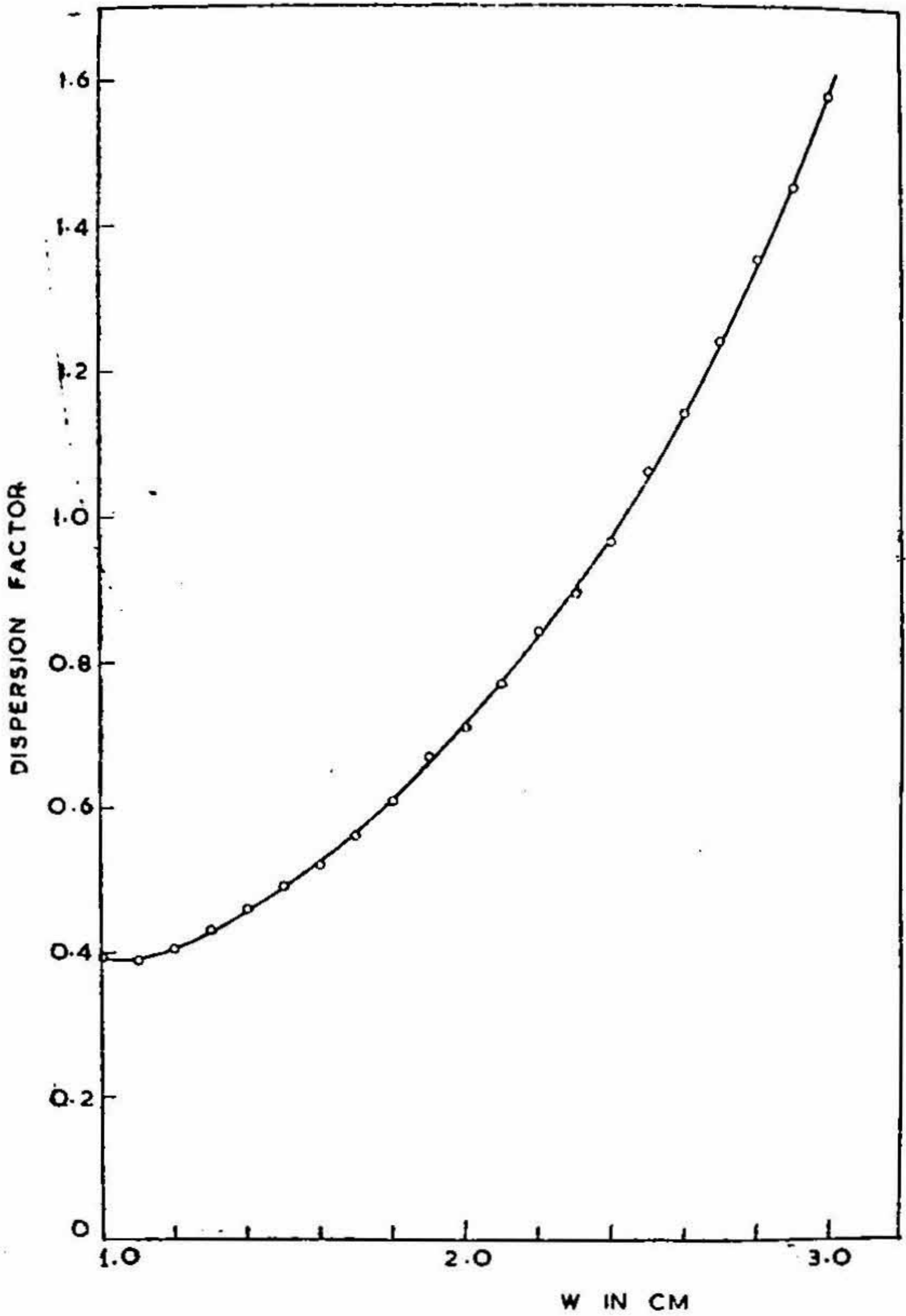


FIG. XVI

Dispersion factor as a function of distance between top and bottom plates.

$\lambda_0 = 10$ cm., $p = 0.165$ cm., $m = 0.11$ cm., $b = 0.159$ cm.

$g = 0.119$ cm., $d = 0.278$ cm., $t = 0.055$ cm., $\alpha = 0.667$ cm.

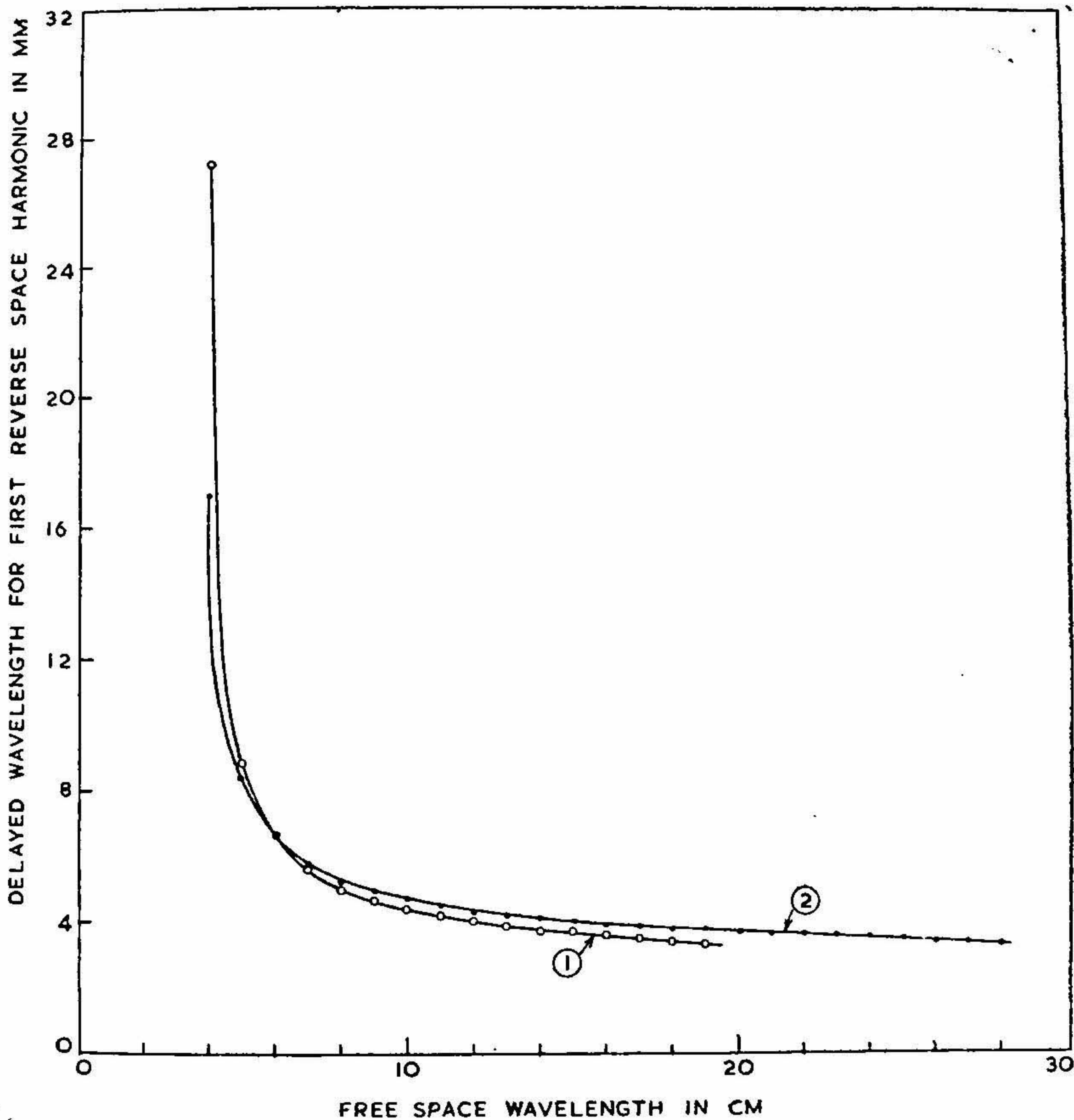


FIG. XVII

Delayed wavelength for first reverse space harmonic as a function of the free space wavelength.

$p=0.165$ cm., $w=1.628$ cm., $m=0.11$ cm., $b=0.159$ cm.
 $g=0.119$ cm., $l=1.509$ cm., $d=0.278$ cm., $t=0.055$ cm.
 $\alpha=0.667$.

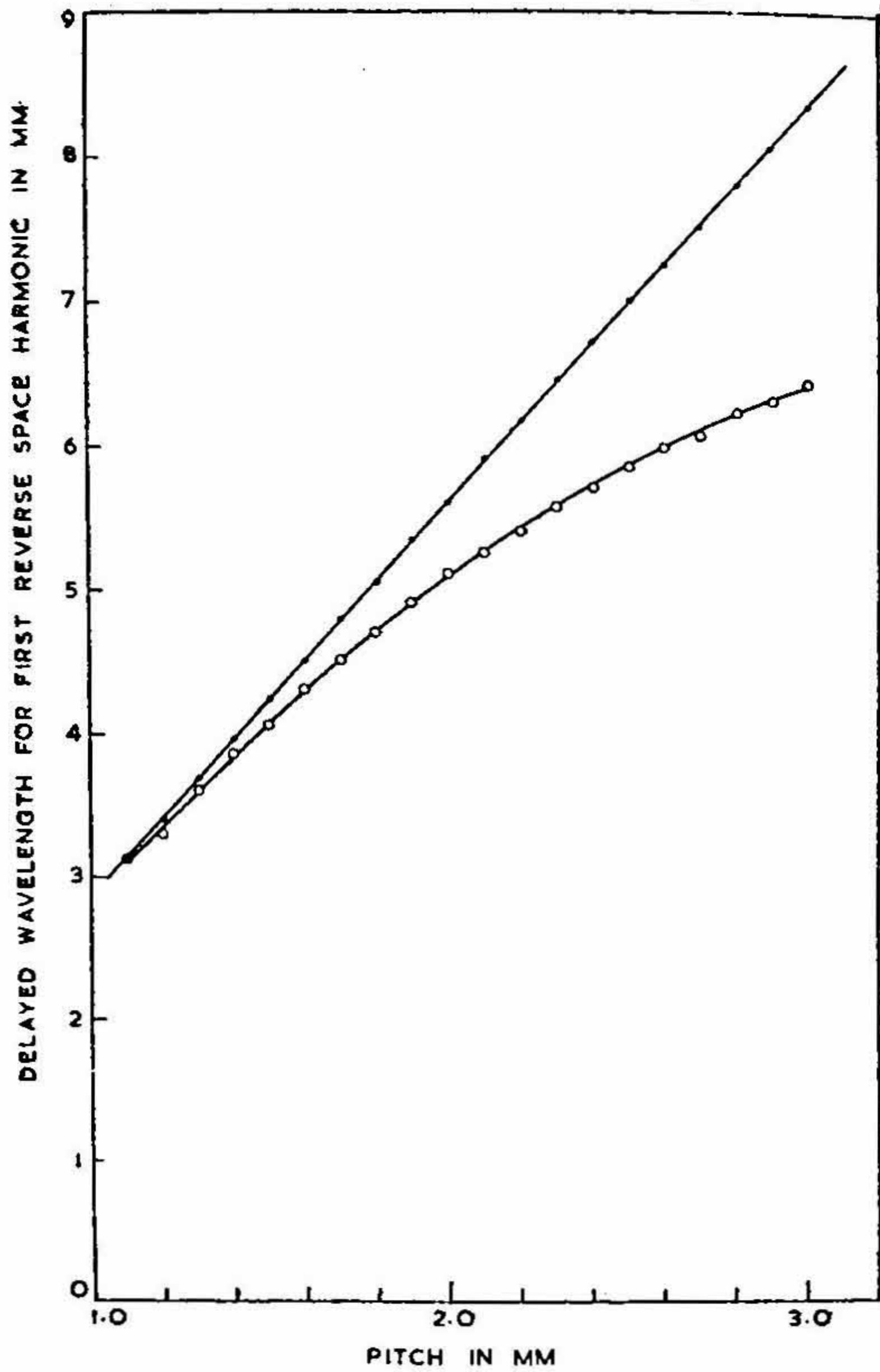


FIG. XVIII

Delayed wavelength for first reverse space harmonic as a function of pitch.

$\lambda_0 = 10$ cm., $w = 1.628$ cm., $b = 0.159$ cm., $g = 0.119$ cm.

$l = 1.509$ cm., $d = 0.278$ cm., $t = 0.055$ cm.

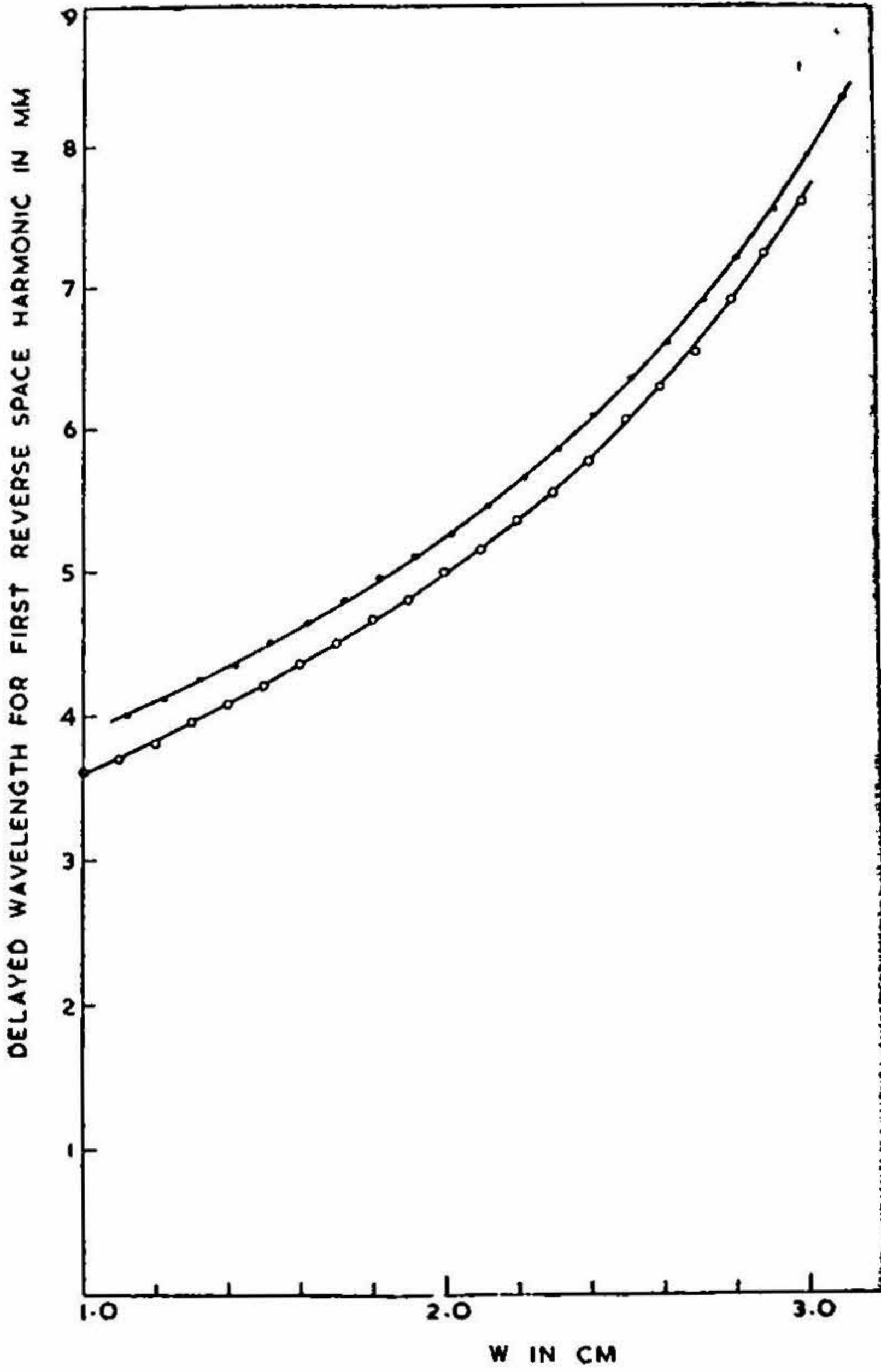


FIG. XIX

Delayed wavelength for first reverse space harmonic as a function of distance between top and bottom plates.

$\lambda_0 = 10$ cm., $p = 0.165$ cm., $m = 0.11$ cm., $b = 0.159$ cm.,
 $g = 0.119$ cm., $d = 0.278$ cm., $t = 0.055$ cm., $\alpha = 0.667$.

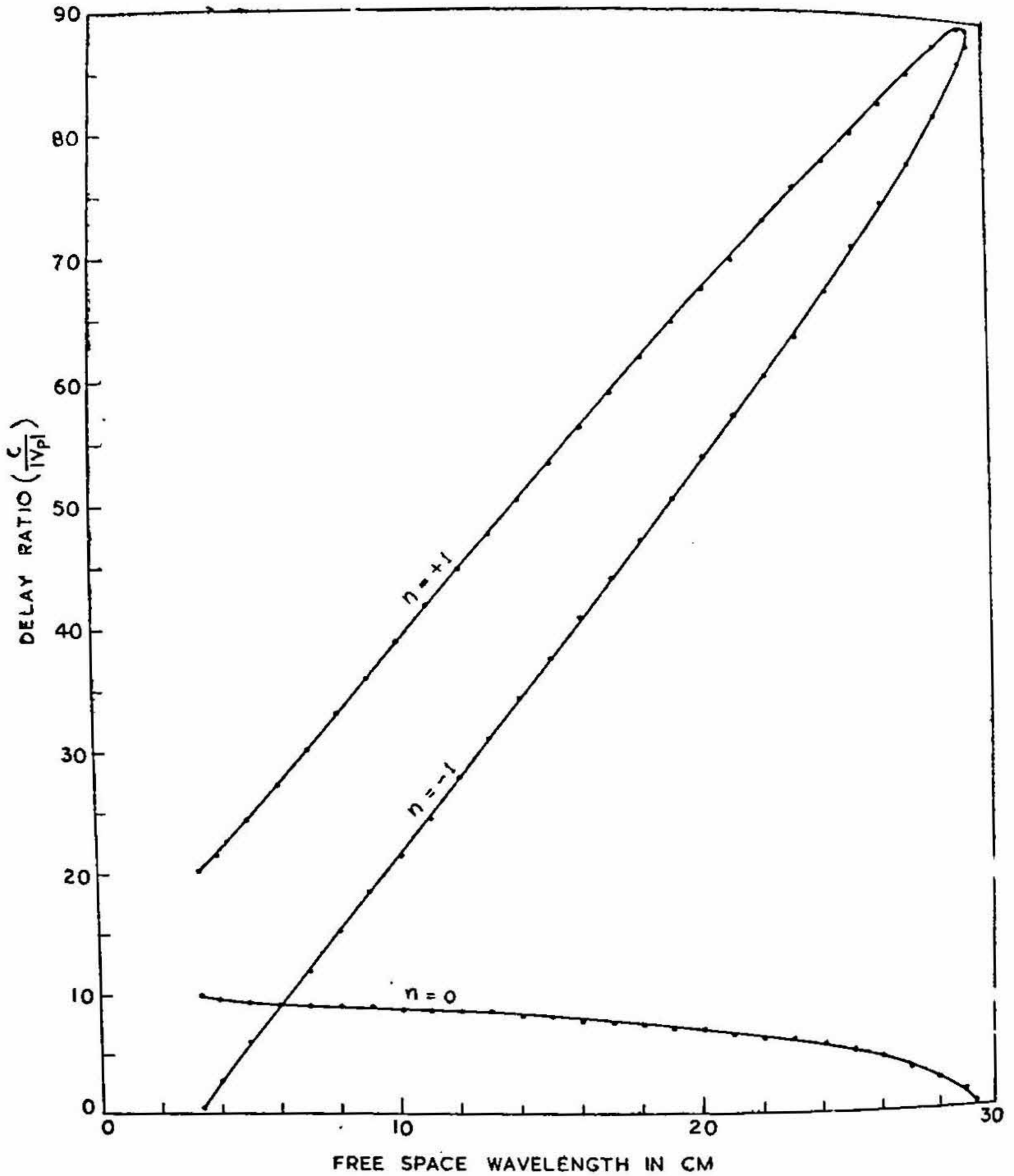


FIG. XX

Delay Ratio as a function of free space wavelength for three different space harmonics ($n=0, -1, +1$).

$p=0.165$ cm., $w=1.628$ cm., $m=0.055$ cm., $b=0.159$ cm.
 $g=0.119$ cm., $l=1.509$ cm., $d=0.278$ cm., $t=0.11$, $\alpha=0.333$.

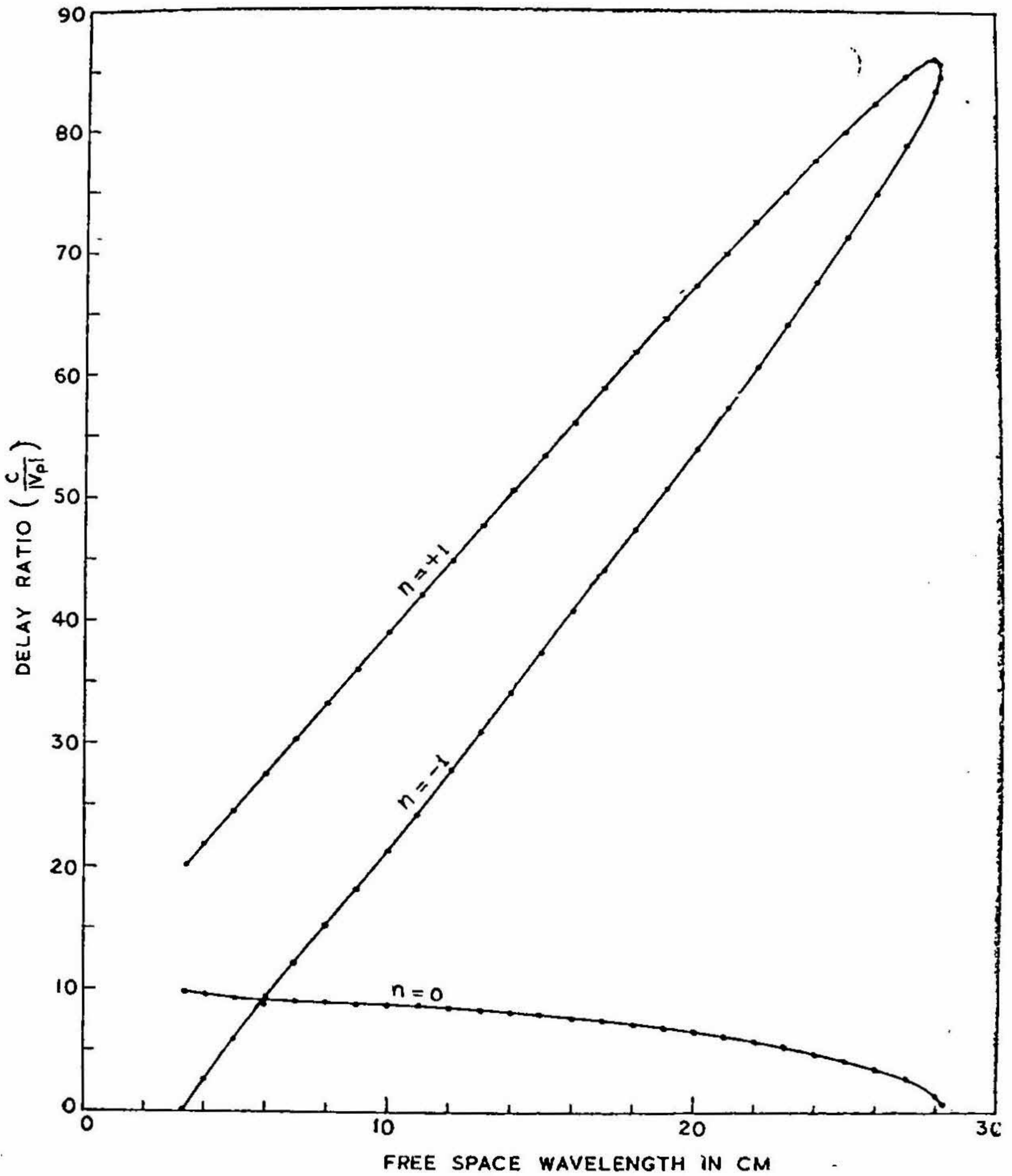


FIG. XXI

Delay Ratio as a function of free space wavelength for three different space harmonics ($n=0, -1, +1$).

$p=0.165$ cm., $w=1.628$ cm., $m=0.0825$ cm., $b=0.159$ cm.
 $g=0.119$ cm., $l=1.509$ cm., $d=0.278$ cm., $t=0.0825$.
 $\alpha = 0.500$.

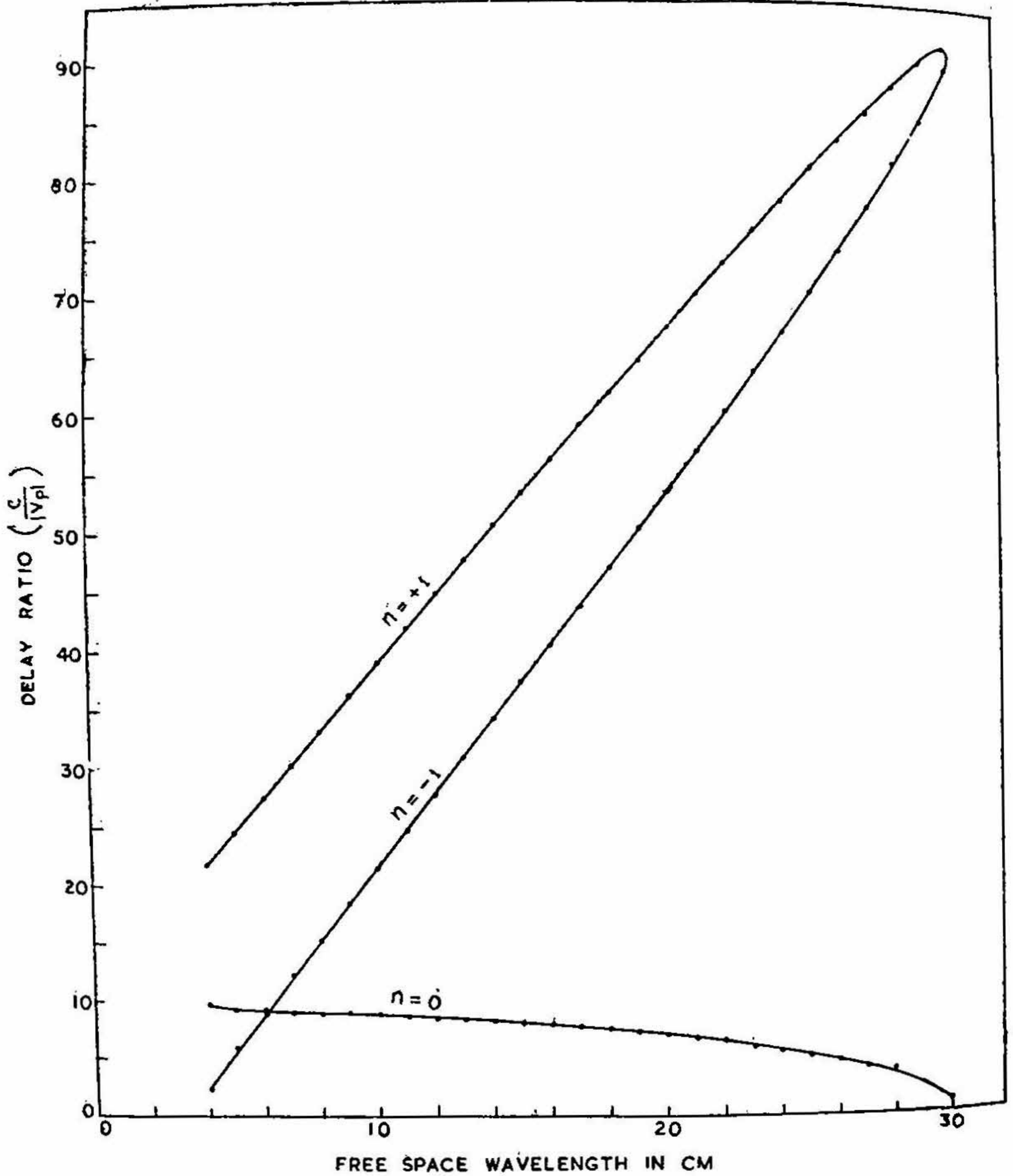


FIG. XXII

Delay Ratio as a function of free space wavelength for three different space harmonic ($n=0, -1, +1$).

$p=0.165$ cm., $w=1.628$ cm., $m=0.11$ cm., $b=0.159$ cm.
 $g=0.119$ cm., $l=1.509$ cm., $d=0.278$ cm., $t=0.055$ cm., $\alpha=0.667$.

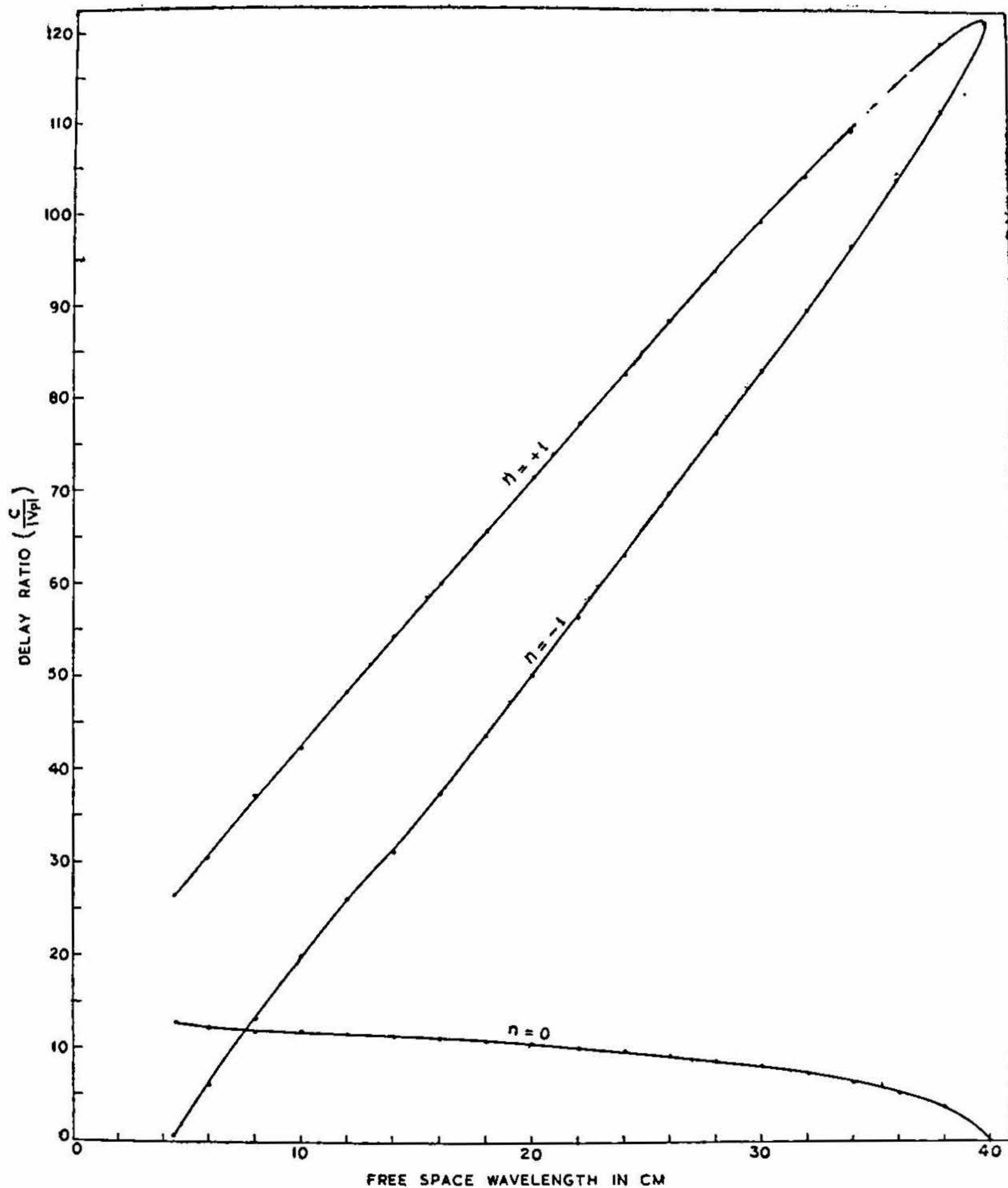


FIG. XXIII

Delay Ratio as a function of free space wavelength for three different space harmonics ($n=0, -1, +1$).

$p=0.165$ cm., $w=2.119$ cm., $m=0.11$ cm., $b=0.159$ cm.
 $g=0.119$ cm., $l=2.000$ cm., $d=0.278$ cm., $t=0.055$ cm., $\alpha=0.667$.

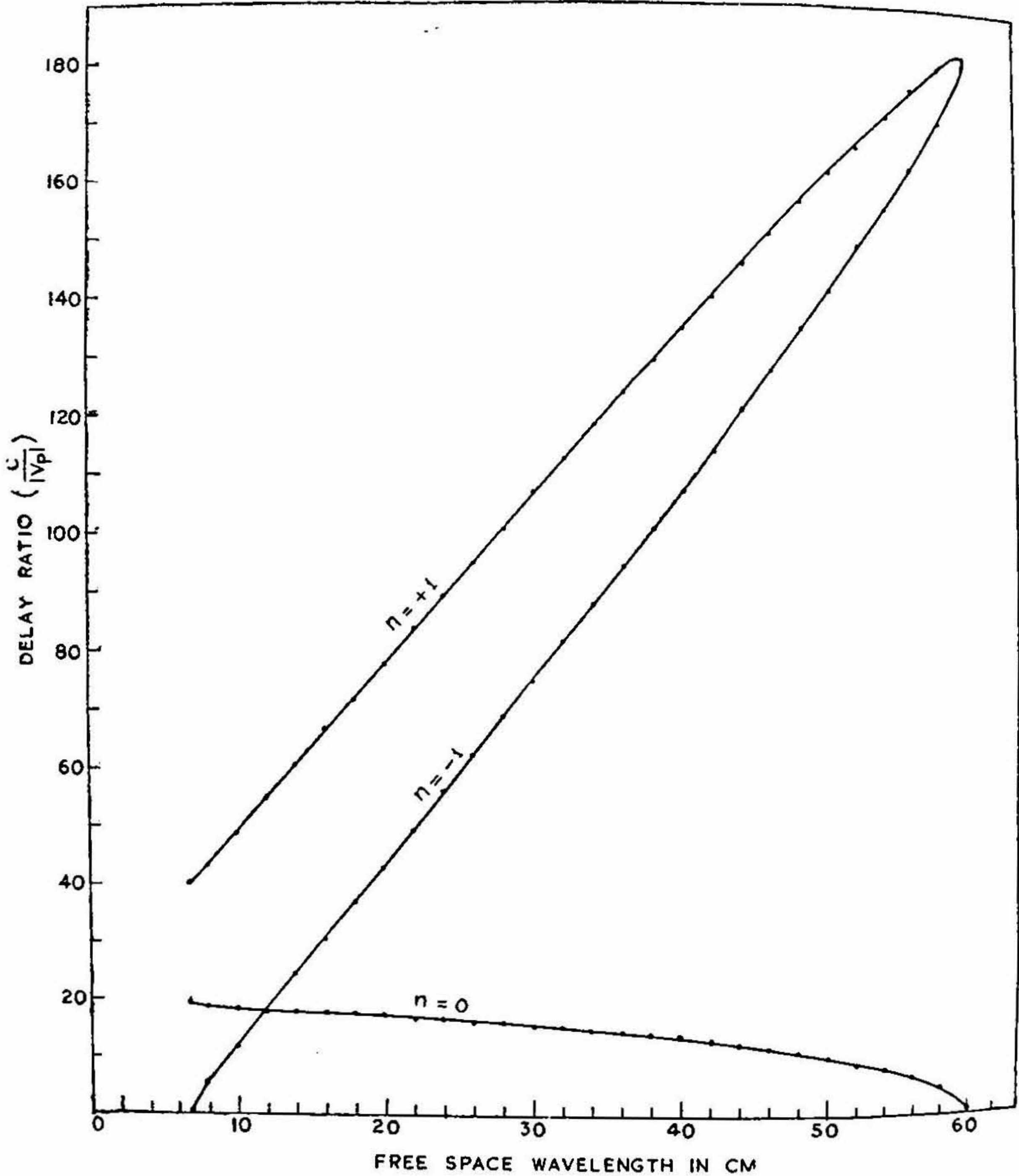


FIG. XXIV

Delay Ratio as a function of free space wavelength for three different space harmonics ($n=0, -1, +1$).

$p=0.165$ cm., $w=3.119$ cm., $m=0.11$ cm., $b=0.159$ cm.,
 $g=0.119$ cm., $l=3.000$ cm., $d=0.278$ cm., $t=0.055$ cm., $\alpha=0.667$.

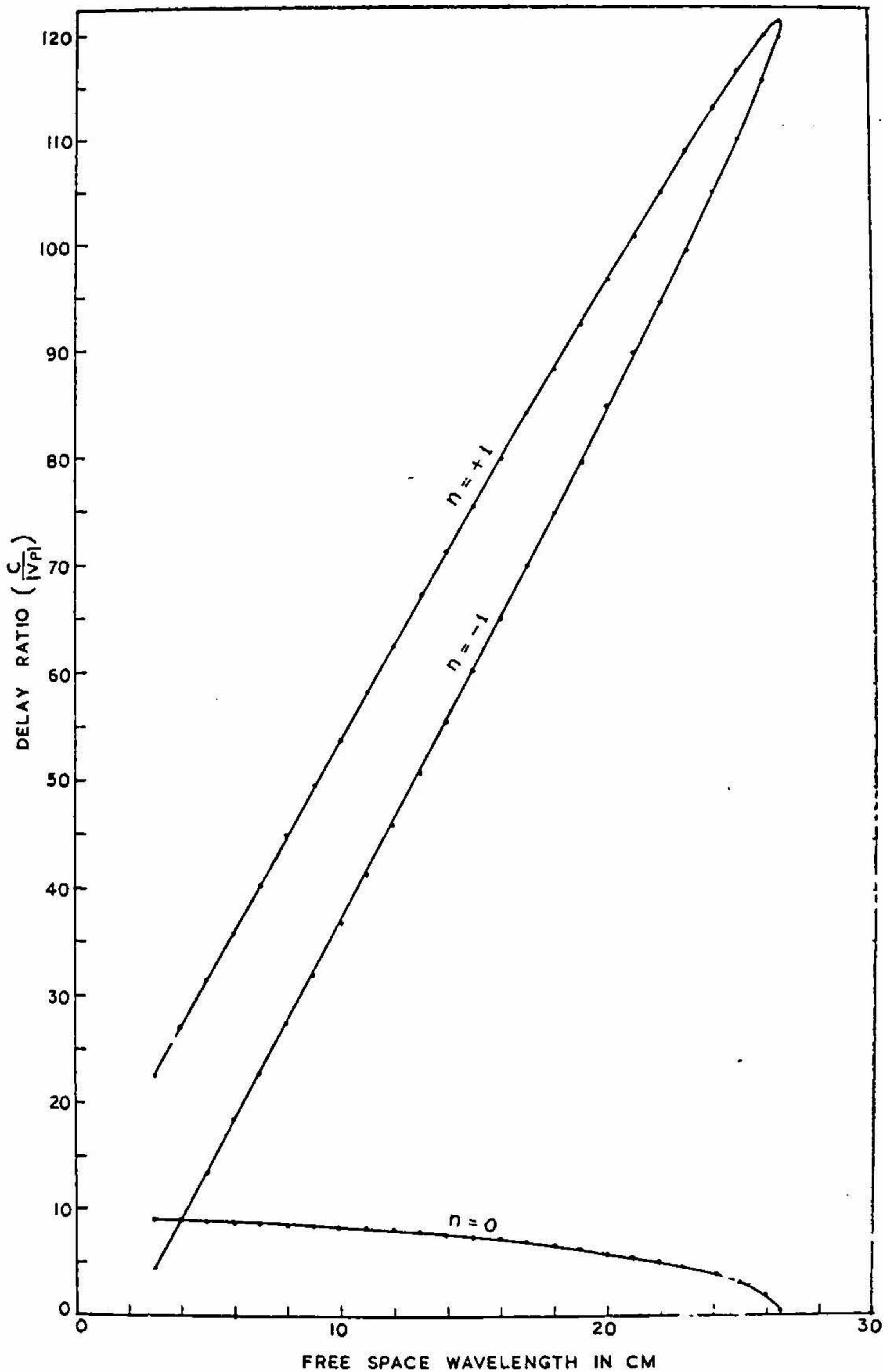


FIG. XXV

Delay Ratio as a function of free space wavelength for three different space harmonics ($n=0, -1, +1$).

$p=0.11$ cm., $w=1.119$ cm., $m=0.055$ cm., $b=0.159$ cm.
 $g=0.119$ cm., $l=1.000$ cm., $d=0.278$ cm., $t=0.055$ cm.
 $\alpha=0.5000$.

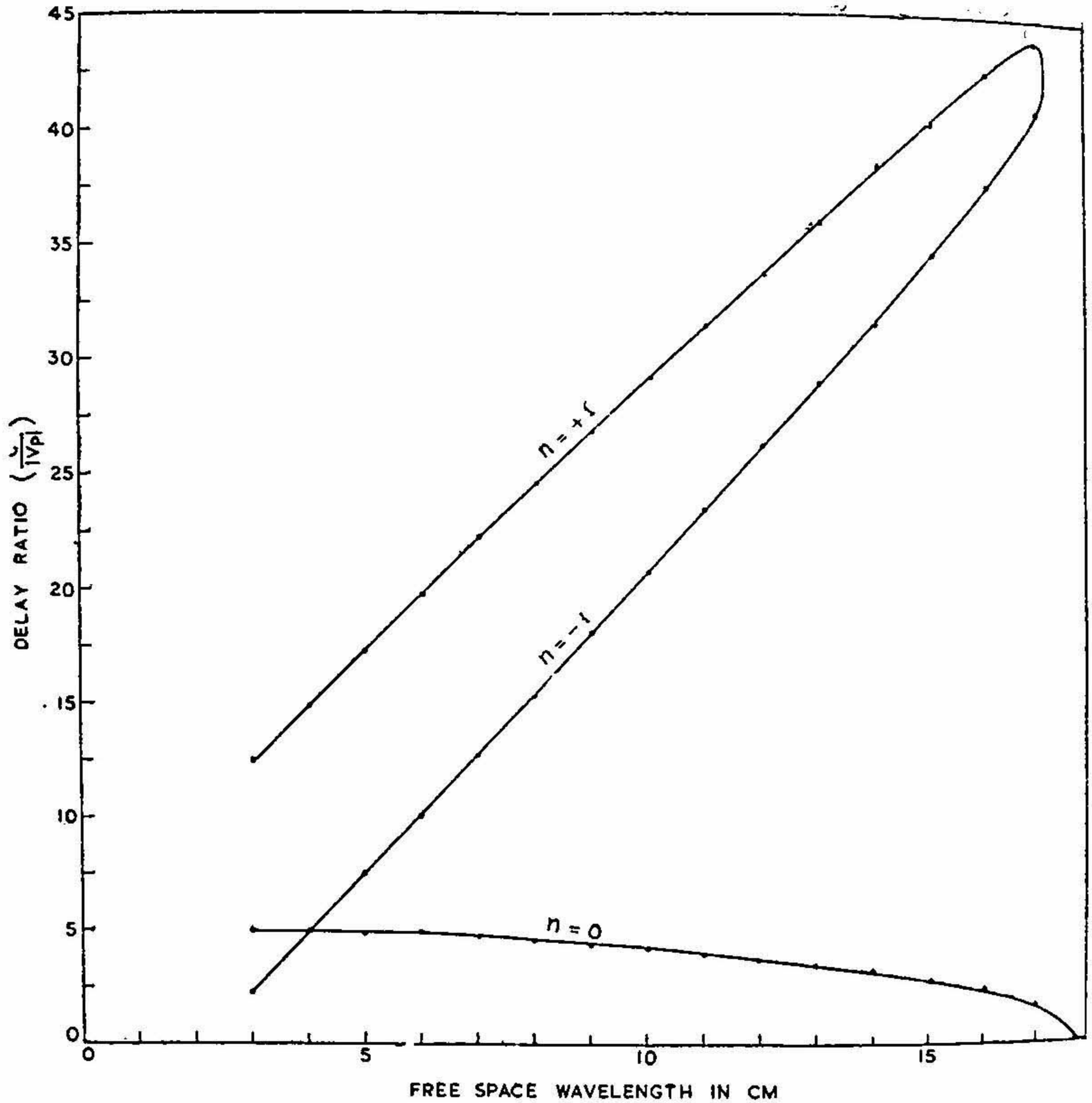


FIG. XXVI

Delay Ratio as a function of free space wavelengths for three different space harmonics ($n=0, -1, +1$).

$p = .200$ cm., $w = 1.119$ cm., $m = .145$ cm., $b = 0.159$ cm., $g = .119$ cm.
 $l = 1.000$ cm., $d = 0.278$ cm., $t = 0.055$ cm., $a = .725$.

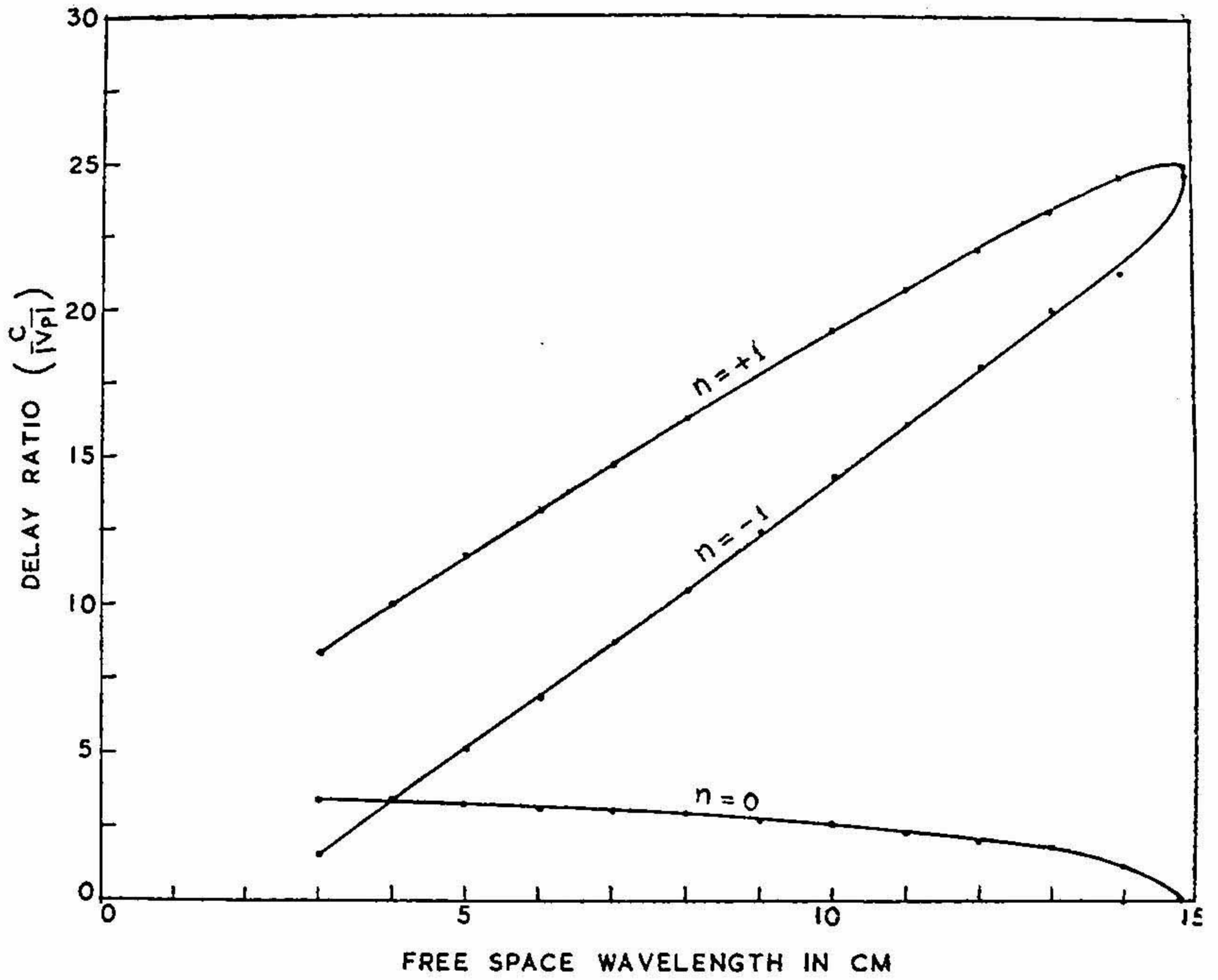


FIG. XXVII

Delay Ratio as a function of free space wavelength for three different space harmonics ($n=0, -1, +1$).

$p=.300$ cm., $w=1.119$ cm., $m=.245$ cm., $b=0.159$ cm.
 $g=0.119$. $l=1.000$ cm., $d=0.278$ cm., $t=0.055$ cm.
 $\alpha=0.817$.

Pitch p and the distance between top and bottom plates W are more significant than the other dimensions in determining the characteristics of the interdigital line. Calculations of the different parameters and their graphical representation have been made in four different cases, namely (i) the free space wavelength (λ_0) corresponding to the frequency of excitation of the structure has been varied from 4 cms to 30 cms, when all dimensions are maintained constant at the values given above, (ii) p is varied from 0.11 cm to 0.30 cm and correspondingly m is varied from 0.055 cm to 0.245 cm and $\lambda_0 = 10$ cms, other dimensions remaining constant, and (iii) W is varied from 1.0 cm to 3.0 cms, other dimensions are maintained constant and $\lambda_0 = 10$ cms, (iv) the delay ratio has been calculated for space harmonics $n = 0, -1$ and $+1$ for the whole pass band for sets of values of p, W and α .

Delay Ratio. The delay ratio has been calculated with the help of equations [1, 2, 4, 6, 13 and 15] and the variation with respect to λ_0, p , and W are shown in Figs. III, IV and V. It is observed from the dispersion characteristic (Fig. III) that the high frequency cut off occurs at a wavelength of nearly 3 cms whether the waveguide approach or the bar line approach is used, whereas in the case of low-frequency cut off, there is considerable difference between the values obtained by two theories. It is considered that the results given by waveguide approach is more accurate at the lower frequencies as the low-frequency cut off is of the waveguide type⁴.

Fig. IV shows that the delay ratio decreases with increasing pitch, but the decrease is more in the case of bar line approach. Fig. V shows that τ decreases with W linearly. The result shows a fine agreement between the two theories at larger values of W .

Low frequency cut-off wavelength. Figs. VI and VII shows the low-frequency cut-off wavelength (λ_1) calculated from eq. [1] and [13] with respect to pitch p and W . It is observed that λ_1 decreases with increasing pitch in both cases but the values of λ_1 differ considerably in the two cases.

Characteristic Impedance. The characteristic impedance of the line is calculated only on the basis of waveguide approach from equations [8] and [9] for different λ_0, p and W and the results are shown in Figs. VIII, IX and X.

Fig. VIII shows that the characteristic impedance is almost constant at about 120 ohms and it starts increasing gradually after 8 cms and tends to infinity at low frequency cut off. For practical purposes, it is desirable that the characteristic impedance remains constant over a wide band of frequencies.

Interaction Impedance. The interaction impedance has been calculated from equation [10] and its variations with λ_0, P and W are shown in Figs. XI, XII and XIII. It is observed that the interaction impedance

increases with p and W . Since the delay ratio decreases with increasing values of p and W , a compromise in design is necessary for pitch and length of fingers. The interaction impedance remains fairly constant from 8 cms. to 18 cms, and tends towards infinity near the low and high frequency cut-offs. Though it is desirable to have a high value of interaction impedance in order to achieve high gain, it is also necessary to have a constant value of interaction impedance over a wide frequency band.

Dispersion Factor. The dispersion factor v_p/v_g has been calculated from the equations [5] and [8] and the variation of v_p/v_g with λ_0 , p and W are shown in Figs. XIV, XV and XVI. It is observed that the dispersion factor tends to infinity near the low and high frequency cut-offs but remains fairly constant from 8 cms to 18 cms which is the useful bandwidth. It is further observed that the dispersion factor remains fairly constant at lower values of pitch and tends towards infinity at $p = 0.30$ cm. It is also seen that the dispersion factor gradually increases with increasing values of W .

Delayed wavelength. The delayed wavelength for first reverse space harmonic is calculated from equations [4], [7] and [15] and the variation of λ_{-1} with respect to λ_0 , p and W is shown in Figs. XVII, XVIII and XIX. λ_{-1} is fairly constant over the whole frequency range except near the high frequency cut-off, but there is an increase of λ_{-1} with increasing values of p and W .

Dispersion curves for different space harmonics. The delay ratio has been calculated for the space harmonics $n = 0$, -1 and $+1$ for eight sets of values for p , W and α , and the dispersion curves showing the variations of delay ratio with free space wavelengths for different harmonics are shown in Figs. XX, XXI, XXII, XXIII, XXIV, XXV, XXVI and XXVII.

It can be observed from the above dispersion characteristics that though the high frequency cut-off occurs when free space wavelength is approximately equal to $2W$, at the lower values of the free space wavelength, the dispersion curves for $n = 0$, and $n = 1$ cross each other. So, it is evident that in order to avoid interaction with the space harmonic $n = 0$, it is better to have the upper cut off frequency corresponding to about $4W$. Also, at the low frequency cut off end, it is observed that dispersion curves for $n = -1$ and $n = +1$ tend to meet each other. There is also a possibility of interaction with the unwanted space harmonic $n = +1$. So, for useful operation, it is desirable to keep the free space wavelength between $4W$ and $8W$ approximately.

CONCLUSION

Design calculations have been made for the interdigital line based on two different approaches. It is expected that these graphical representations will be helpful in designing an interdigital line. Especially, the graphs showing the variations of different parameters with important dimensions, will serve as a ready reference in choosing the dimensions.

ACKNOWLEDGEMENT

The author expresses her gratitude to Dr. (Mrs) Rajeswari Chatterjee and Mr. S. K. Chatterjee for guidance and suggestion of the problem. She is also thankful to the University Grants Commission for the award of a Senior Research Fellowship.

LIST OF SYMBOLS

τ	Delay Ratio.
λ_{-1}	Delayed wavelength for first reverse space harmonic.
Z_0	Characteristic impedance of the interdigital line.
K_{-1}	Interaction impedance for first reverse space harmonic defined at the edge of fingers.
v_p/v_R	Dispersion factor.
λ_1	low frequency cut-off wavelength.
λ_2	high frequency cut-off wavelength.
α	ratio of gap width to pitch.
C	Dimensionless factor proportional to capacity of fingers.
L	Dimensionless factor proportional to inductance of fingers.
γ_0	Capacity per unit length between a finger and ground.
γ'	Capacity per unit length between adjacent fingers.
λ_0	Free space wavelength in cms corresponding to the operating frequency.
β_0	Propagation constant in free space.
β	Propagation constant in the line in Z-direction.
β_n	Propagation constant in Z-direction for the n th order space harmonic.
γ	Propagation constant in Y-direction.
ω	Angular frequency.
μ	Permeability of free space.
ϵ	Permittivity of free space.
n	Order of space harmonics.
v_g	Group velocity.
v_p	Phase velocity.
Y	Admittance for TEM wave along the structure.
ψ	Fundamental phase shift ($= 2\beta p$).

REFERENCES

1. Leblond A. and Mourier, G. ... "Study of bar lines of periodic structure for UHF electron tubes", *Ann. Radioelec.*, 1954, 19, 180, 311.
2. Fletcher, R. C. ... "A broadband interdigital circuit for use in travelling-wave type amplifiers", *Proceedings of the Institute of Radio Engineering*, 1952, 40, 951.
3. Arnand, T. ... "Theory of Bar lines", "Circuits for travelling wave crossed field tubes" and "Measurements", *Crossed-field Microwave Devices, Vol. 1*, Edited by E. Okress, Academic Press, New York, 1961.
4. Moats, R. R. ... "The Interdigital Line as a waveguide", *Crossed-field Microwave Devices, Vol. 1*, Edited by E. Okress, Academic Press, New York, 1961.